MODELING AND PERFORMANCE ANALYSIS OF MULTIMEDIA TRAFFIC OVER COMMUNICATION NETWORKS

By

KYUNGWOO KIM

A DISSERTATION PRESENTED TO THE GRADUATE SCHOOL
OF THE UNIVERSITY OF FLORIDA IN PARTIAL FULFILLMENT
OF THE REQUIREMENTS FOR THE DEGREE OF
DOCTOR OF PHILOSOPHY

UNIVERSITY OF FLORIDA

2012

I dedicate this work to my parents and my wife.

ACKNOWLEDGMENTS

First and foremost, I would like to express my sincere gratitude to my advisor, Dr. Haniph Latchman. I have benefited from his patience, guidance, and great kindness, I wish to say a heartfelt thank you to him. His belief in my ability has made me achieve the goals that I pursued. This work would not have been possible without his encouragement and fostering my effort. Looking back, many times I was lost and frustrated. Dr. Latchman always listened to my words and encouraged and giuded me on the right path. Again, I deeply thank him for his invaluable advice. I also would like to thank all the members of my committee (Dr. Janise McNair, Dr. Richard Newman, Dr. Antonio Arroyo) who gave me their interests and helpful suggestions on my research. When I started my academic career at University of Florida, I took the Dr. McNair's class. Deep knowledge and keen insight into the area of stochastic analysis and probability theory that I have been given from her class contributed greatly to the success of the research. Dr. Arroyo broadened my horizons and gave a very helpful insight into problem nature that I frequently faced with during my academic times at University of Florida. I also thank Dr. Newman for his kind advice and numerous discussions we had. I also thank all of my colleagues, especially members of the Laboratory for Information Systems and Telecommunications (LIST), Mr. Jungeun Son and Mr. Youngjoon Lee, for their helpful discussions on academic questions that arise in many situations during my times at LIST laboratory.

As always, I thank to my parents and parents-in-law with all my heart for their endless love and support during the long journey. And I am deeply indebted to my wife Bomin. She deserves special praise, as she always has been with me and patiently supported my research and Ph.D. study. The love I have been given from her and my family makes my life wonderful. It goes far beyond the words I can express.

TABLE OF CONTENTS

LIST OF TABLES

LIST OF FIGURES

Abstract of Dissertation Presented to the Graduate School
of the University of Florida in Partial Fulfillment of the
Requirements for the Degree of Doctor of Philosophy

MODELING AND PERFORMANCE ANALYSIS OF MULTIMEDIA TRAFFIC OVER COMMUNICATION NETWORKS

By

Kyungwoo Kim

May 2012

Chair: Haniph A. Latchman
Major: Electrical and Computer Engineering

Applications of multimedia traffic over various communication channels need to share physically limited bandwidth efficiently and at the same time guarantee Quality of Service (QoS). As the size of multimedia data increases to quarantee a high quality, transmission delay also increases and this results in poor QoS over communication networks. For guaranteed QoS and low transmission delay in communication networks which provides an integrated multimedia service, it is desirable to study the statistical characteristics of multimedia traffic and is important to obtain an analytical and tractable model of compressed MPEG data. This dissertation presents a statistical approach to obtain an MPEG frame size model and estimates throughput and transmission delay over communication networks.

For the study of multimedia traffic characteristics, MPEG-2 frames are extracted from typical DVD movies. To obtain candidate distributions, a probability histogram based on the Freedman-Diaconis method, which is used as a decision rule for a bin size, is considered and both single distributions and a mixed type distribution are also taken into account. In the single distribution case, distribution parameters are obtained from empirical data using the maximum likelihood estimation (MLE) method. The best fitted model for the multimedia traffic studied was found to be a Lognormal distribution.

However, with this single distribution, we cannot explain the inherent multimodality clearly observed in the empirical multimedia frame data. Thus a Hyper-Gamma

distribution is considered as an alternative model to explain its inherent multimodality. The Hyper-Gamma distribution parameters are obtained by means of an expectation maximization algorithm based on the K-means algorithm and a posteriori probability. Furthermore, the Bayesian Information Criterion (BIC) is used as a goodness of fit criterion. Single probability distributions are also considered to demonstrate the superiority of the proposed model in fitting MPEG-2 frame data. This dissertation shows that the Hyper-Gamma distribution is a good candidate for a stochastic model for MPEG-2 frame data.

After obtaining a statistical model for multimedia traffic, the Hyper-Gamma service time distribution has been applied to network systems which are composed of nodes with a finite and infinite capacity and connected in tandem. The throughput for the infinite capacity system is equal to the average arrival rate because of the assumption for a Poisson arrival process and Burke's theorem, meanwhile the total delay is represented in terms of the average arrival rate, and the first and second moments of the Hyper-Gamma service time distribution. But, in case of the finite capacity system, the throughput at each node is represented in a product form of the arrival rate to that node and one minus its blocking probability. Furthermore, the delay in each node depends on the total time spent in the previous node. Therefore, this dissertation predicts throughput and transmission delay for multimedia traffic from the estimated Hyper-Gamma service time distribution and this result will be useful in the performance analysis of network systems based on multimedia traffic.

CHAPTER 1
INTRODUCTION

1.1 An Overview of Multimedia Traffic

Over the past few years communication networks have rapidly evolved to satisfy the customer's needs for integrated services such as voice over IP, personal or industrial video, and entertainment multimedia, etc. Thus, multimedia traffic has become one of the major sources of network traffic loads. Moreover, multimedia services such as real-time streaming video, online games, IP-TV, and Digital Multimedia Broadcasting (DMB) are sensitive to transmission delay and a demand for high quality of service (QoS).

Especially, in case of a home network which is defined as a small area network within a residential unit, a lot of home network standards and technologies have been developed to improve throughput, mitigate transmission delay effects, and enhance QoS for multimedia traffic which allow the use of home HDTV, IPTV, interactive online games, etc. The type of home networking standards are as follows: Home Phoneline Networking Alliance (HomePNA) which provides home network system over a typical phoneline, Multimedia over Coax Alliance (Moca) which uses the equipped coaxial cable over home networks, HomePlug Powerline Alliance (HomePlug AV) which uses installed powerlines, IEEE 802.11n standard which is an amended version of 802.11x, Ultra Wideband (UWB) which employs the IEEE 802.15.3a standard, and G.hn which is developed under the International Telecommunication Union (ITU-T) and supports networking over power lines, phone lines and coaxial cables.

Moreover, in the design of systems that transmit multimedia information through a wired or wireless channel, taking into account the physical limitations of channel characteristics, it is desirable to have an analytical and tractable model of multimedia traffic characteristics for guaranteed QoS and efficient management of network

bandwidth in communication networks, since the frame size of MPEG data is relatively large and fluctuates considerably.

In response to the evolution of network technologies and the feature of multimedia traffic, researchers have proposed a series of analytical MPEG source models in the literature. Nomura and colleague [1] introduced the first order AutoRegressive (AR) model, which estimated the burst of video sources with measured autocorrelation, coefficient of variation, and probability distribution. The result of their study is that the statistical characteristic of Variable Bit Rate (VBR) video information follows a bell-shaped distribution. But Nomura's model now no longer fits a single general video source. [2, 3] Heyman, Frey, Lee, and O. Rose have suggested a gamma distribution-based model. O. Rose [4] suggested a layered modeling scheme for MPEG video traffic. According to Rose's layered model, MPEG video traffic is composed of three layers: Cell layer, Frame layer, and GOP layer; and the statistical model of the frame and Group of Pictures (GOP) size can be estimated by Gamma or Lognormal density function. Based on Rose's layer model, it is possible to obtain an outline of a variety of stochastic modules and the description of how they interact in the case of video traffic. But there are difficulties in finding traffic classes for MPEG video traffic. The statistical characteristics of the Heyman's Gamma Beta AutoRegressive (GBAR) model [5, 6] have a geometric form of autocorrelation function and a Gamma (or Negative-Binomial) marginal distribution. Heyman's research is conducted based on a long (30 min) sequence of real video teleconference data and the GBAR model is tractable because it has just three parameters to be estimated. However the GBAR model is not adequate to fit general MPEG data because Heyman built the GBAR model based only on the VBR videoconference data. [3] Lee [7] suggested a sum of two gamma density functions model, in which he added individual gamma density functions, normalized them, and obtained parameters using a nonlinear least square algorithm. Lee's model is simple and easily dealt with but, sometimes, has weakness in parameter

estimation, so that it often has a poor performance in fitting to various empirical data. Frey [3] proposed a GOP GBAR model, which is an upgraded version of Heyman's GBAR model. Frey and his colleague suggested that the size of an MPEG B-frames, P-frames, and I-frames could be modeled as one gamma random variable, the sum of two gamma random variables, and the sum of three gamma random variables, respectively. The GOP GBAR model is also simple and analytical but, with the above Gamma distribution-based models, cannot explain the multimodal property observed in the empirical MPEG data histograms. The multimodal property also arises in an empirical histogram of MPEG-4 and H.263 frame data and online game traffic. [8, 9]

1.2 Network System Modeling

A network system can be considered as systems of flow. A number of packets are transferred through one or more channels which are limited in capacity from one node to another. In this kind of situation, a packet service rate in a node has to be always bigger than a packet arrival rate into a node to avoid a packet loss or guarantee the stable system flow. However, if the packet arrival rate is bigger than the packet service rate, then the packet begins to overflow and can be blocked or result in packet loss at the node. Moreover, the arrivals or the size of packets often arise in an unpredictable fashion. Thus, conflicts for the use of the channel are inevitable, queues of waiting will arise, and these environments bring about the network traffic loads. When one would like to predict or specify the dynamics of systems of flow, and analyze the performance of network systems, the inherent property of randomness in the packet arrival process and service time distribution must be considered.

Another consideration of network systems is a performance of flow in terms of throughput and delay. Before describing the throughput and delay, it is necessary to specify an average packet arrival rate and average service rate. The average arrival rate and average service rate are defined as the expected number of the packet arrivals per unit time and the expected number of packets in service per unit time, respectively.

Generally, throughput of a network system measured in bits/second or frame/second is defined as the average rate with which packets are successfully transferred through the channel, so actual throughput is a product of a packet departure rate and non-blocking probability. Delay can be considered as a sum of average waiting times in queues and service times in network nodes.

The simplest and conventional way of approaching this kind of dynamic systems is the queueing theory. According to the basic queueing system (i.e. M/M/1 queue), the arrival process is a Poisson process and the service time follows an exponential distribution with a single server. But when we venture beyond the classical network model (i.e. M/M/1 queue) into the more general and empirical world, then rather complex phenomena arise, which implies the arrival process and service time distribution is not always a Poisson process and an exponential distribution, respectively. [10–12]

Generally, a method of analytically tractable modeling of network systems to evaluate its performance consists of two parts. The first part is to find statistical characteristics of network traffic; that is, which probability density function can specify the statistical property of traffic flow, and the other part is to figure out a relationship between the stochastic model and its resulting traffic characteristics such as throughput over a network channel or transmission delay. Moreover, the MPEG2 standards follows three types of frame (i.e. Intra-coded frame, Predictive frame, and Bidirectional frame) which has random size of frames. In a queueing viewpoint, a different packet size is directly related to the average service rate or its service time distribution. Therefore, there is an essential need to investigate a statistical model of the MPEG frame size to determine its service time distribution for MPEG traffic flow. Also, it is inevitable to take into account throughput and transmission delay over communication networks based on the queueing analysis. This dissertation proposes such a model which can be used for a performance analysis for communication networks based on multimedia traffic.

1.3 DVD Video Stream: MPEG-2 Standards

Nowadays, the most pervasive optical disc storage medium which can store multimedia data is DVD. DVDs can store more than six times as much data compared with previous trends storage media which are called CDs (Compact Disc). Moreover, DVD-Video becomes the dominant form of home video distribution worldwide. This section gives a brief overview of a DVD video format in which MPEG-2 standards is most widely used. Note that DVD video data used in this research were extracted from commercial DVDs. This work is done for academic purposes only and there were no edits, distributions, or collections after this research.

MPEG-2 standards provide three types of main frames. Intra coded frames (I-frames) are directly encoded from the information in the picture itself; that is, the encoding process of I-frames is independent of all other frames and uses transform coding with only moderate compression. I-frames provide random access points to the encoded video sequence where decoding can begin. Predictive coded frames (P-frames) are encoded by using motion compensation, which is called forward prediction, with respect to the most recent I-frames or P-frames. The compression rate of P-frames is more substantial than I-frames. Bidirectional-predictive coded frames (B-frames) are encoded by using a bidirectional prediction relative to both the previous and subsequent I-frames or P-frames as a reference frame. B-frames provide the highest rate of compression of the three frame types; however, they have the largest time to encode. B-frames cannot be used as references for prediction. The organization of the three frames in a sequence is very flexible. [3, 13–16]

The MPEG-2 video stream structural hierarchy is as follows: block, macroblock, slice, picture, GOP, video stream sequence. Generally, a digital image is a set of 2-dimensional picture elements which are called pixels, and pixels become the smallest unit of image information. Since raw image data have an enormous amount of information, image compression technique is inevitable to represent a digital image.

One of the most commonly used methods for image compression is the discrete cosine transform (DCT). Based on the DCT coding scheme, compressed data is stored in a block which is a set of 8 by 8 array of pixels or 64 coefficients of the DCT. The block is called the fundamental coding unit in the MPEG standards. The MPEG-2 standards defines a macroblock as a 16 by 16 pixel segment in a frame, in other words, 4 blocks of luminance and 2 blocks of chrominance. The macroblock plays a role of a basic unit for motion compensation in the MPEG-2 standards. An arbitrary number of sequences of macroblocks which stand in the same row are called a slice, in which macroblocks are aligned from left to right and top to bottom. A picture is defined as encoded image data. In general, a picture is identical to a frame, which works as the primary coding unit of a video sequence in MPEG-2 stream. The encoded frames or pictures in MPEG-2 are arranged in groups of pictures (GOP). The GOP always starts with an I-frame; the P-frames and B-frames are inserted into the sequence. Therefore, a general structure of the GOP can be represented by a series of frames, IBBPBBPBBPBB, but this is not a regular format. A video stream sequence is the highest syntactic structure of encoded video streams. It starts with a sequence header which is followed by one or more contiguous coded frames (or a group of pictures), and ceases by a sequence end code. [7, 14–17]

The traffic modeling of the MPEG frames with single distributions is described in Chapter 2. Another approach to figure out the statistical characteristics of multimedia traffic using the Hyper-Gamma distribution is introduced in Chapter 3. Chapter 4 briefly demonstrates some methods for an analysis of multimedia traffic and Chapter 5 presents an approach to the performance analysis for network systems based on multimedia traffic. Finally, Chapter 6 conclude this dissertation with results for the performance of network systems such as throughput and delay which have nodes connected in series.

CHAPTER 2
TRAFFIC MODELING OF MPEG FRAMES WITH SINGLE DISTRIBUTIONS

2.1 An Overview of a Statistical Approach to MPEG Frames

For guaranteed quality of service (QoS) and sufficient bandwidth in communication networks which provides an integrated multimedia service, it is important to achieve an analytical model for compressed MPEG data. Chapter 2 presents a statistical approach to an MPEG frame size model to increase network traffic performance in communication networks. MPEG frame data are extracted from commercial DVD movies and empirical histograms are considered to analyze the statistical characteristics of MPEG frame data. Six candidates of probability distributions are considered here and their parameters are obtained from empirical data using the Maximum Likelihood Estimation (MLE). Chapter 2 shows that the Lognormal distribution is the best fitted model of MPEG-2 total frames as a single probability distribution.

Multimedia information is stored and transmitted as compressed data in a device and channel, respectively. Two types of commonly used compression methods are MPEG-2, which is the second version of standards developed by the Moving Pictures Expert Group (MPEG) and H.264, which is also known as MPEG-4 Part 10 or MPEG-4 AVC (Advanced Video Coding). These two encoding methods are widely used commercially. For example, Blu-ray discs and digital HDTV use both MPEG-2 and MPEG-4 AVC as encoding method. An MPEG-2 format is used in current commercial DVD movies. But if compressed MPEG-2 or MPEG-4 AVC (H.264) data is transmitted through a wired or wireless channel, taking into account the physical limitations of channel characteristics, the transmission must guarantee QoS, which means that the channel must provide sufficient throughput and tolerable transmission delay. It is therefore important to achieve an analytical and tractable model for a distribution of compressed MPEG data because the frame size of MPEG data is relatively massive and fluctuates considerably.

A simple stochastic model for the MPEG-2 frame size is proposed in Chapter 2 to improve bandwidth utilization and to reduce transmission delay. In order to obtain the model that well fits empirical data, six different probability distributions in which their parameters are determined by an Maximum Likelihood Estimation (MLE) method is considered to compare and analyze the statistical characteristics of MPEG-2 frame traffic. Chapter 2 presents that the best model for the distribution of the total MPEG-2 frame size is a Lognormal distribution by means of a Mean Squared Error (MSE) method.

2.2 Statistical Modeling of MPEG Frames with Single Distributions

This section presents an experimental analysis of the statistical characteristics of MPEG-encoded commercial DVD movie frame data and shows that the application of the result to empirical data is good enough to specify the characteristics of MPEG-2 total frame data. As mentioned previously, the procedure of the MPEG traffic modeling is generally composed of two parts. The first part is to find the statistical characteristics of MPEG traffic and build a precise model for a statistical analysis, and the other is to figure out a relationship between the statistical model and its traffic characteristics. Chapter 2 and Chapter 3 are especially focused on the first part, a statistical modeling of MPEG traffic which is based on the B-frames, P-frames, I-frames, and total frames. The frame size model of MPEG traffic has a similar statistical characteristic (i.e. the shape of pdf) of a Gamma distribution, a Lognormal distribution, a Rayleigh distribution, a Weibull distribution, a Nakagami distribution, and a Rician distribution. Chapter 2 presents six similar shapes of probability distributions and compares their pdfs and cdfs with that of original data.

The first step of a statistical analysis for empirical data is to build an empirical histogram. Conventionally, making a histogram is a natural and fundamental way of representing a set of empirical data drawn from a real world and one can afford to estimate a statistical characteristic of data with this technique. However, when we are

trying to use a method of the histogram, there needs a careful consideration; in order to make a histogram one must decide the number of bins to use. As an extreme example, we can consider the following case. There is a set of data (e.g. 10000 samples) drawn from the Gaussian distribution. If we put all samples in one bin of the histogram, then we can see that the statistical characteristics of empirical data looks like a uniform distribution, meanwhile if we choose the same number of bins of the histogram as the number of empirical data samples (i.e. an analysis with raw data itself), it could not be easy to catch out the inherent statistical characteristics. Therefore, this dissertation uses a Freedman-Diaconis method as a decision rule for a bin size to figure out a probability histogram from frame data: [18]

$$\text{Bin\_Size} = 2 \times \text{IQR}(x) \times n^{-1/3} \tag{2–1}$$

where the $IQR(x)$ is the interquartile range of empirical data, i.e. the difference between the 75th and 25th percentile of empirical data and n is the number of observations in sample x. The Freedman-Diaconis technique was based on the goal of minimizing the sum of squared errors between the histogram bar height and the probability density of the underlying distribution which gave the $n^{-1/3}$ part of the equation. The use of $2 \times IQR(x)$ as a measure of spread was determined from their empirical experiments.

The parameters which specify the statistical characteristics of each probability distribution are estimated by the MLE method. In addition, the MSE method is selected to evaluate the best fitted model for the distribution of the MPEG frame size. The followings are density function formulae of each candidate distribution. For a Gamma distribution,

$$f_{GAM}(x) = \frac{x^{k-1}e^{-x/\theta}}{\theta^k \Gamma(k)} \qquad x > 0 \tag{2–2}$$

where k is a shape parameter and θ is a scale parameter. Both parameters are positive and real. For a Lognormal distribution,

$$f_{LOGN}(x) = \frac{1}{x\sigma\sqrt{2\pi}} e^{-\frac{(\ln x - \mu)^2}{2\sigma^2}} \qquad x > 0 \tag{2–3}$$

where μ is a location parameter (mean) and σ is a scale parameter (standard deviation). For a Nakagami distribution,

$$f_{NAKA}(x) = \frac{2\mu^{\mu}}{\omega^{\mu}\Gamma(\mu)} x^{2\mu-1} e^{-\mu x^2/\omega} \qquad x > 0 \tag{2–4}$$

where μ is a shape parameter and ω is a spread parameter. Both parameters are positive and real ($\mu \geq 0.5$). For a Weibull distribution,

$$f_{WEIB}(x) = \frac{k}{\lambda}\left(\frac{x}{\lambda}\right)^{k-1} e^{-(x/\lambda)^k} \qquad x > 0 \tag{2–5}$$

where λ is a scale parameter and k is a shape parameter. Both parameters are positive and real. For a Rayleigh distribution,

$$f_{RAYL}(x) = \frac{x}{\sigma^2} e^{-\frac{x^2}{2\sigma^2}} \qquad x > 0 \tag{2–6}$$

where σ is a scale parameter and it is positive and real. For a Rician distribution,

$$f_{RICI}(x) = \frac{x}{\sigma^2} e^{-\frac{x^2+\nu^2}{2\sigma^2}} \mathrm{I}_0\left(\frac{x\nu}{\sigma^2}\right) \qquad x > 0 \tag{2–7}$$

where $\mathrm{I}_0\left(x\nu/\sigma^2\right)$ is the modified Bessel function of the first kind with order zero. σ is a scale parameter ($\sigma \geq 0$ and $\nu \geq 0$).

Heyman and Frey already proposed a gamma-based frame size model. Especially, Frey and his colleague suggested that the size of MPEG B-frames, P-frames, and I-frames could be modeled as one gamma random variable, the sum of two gamma random variables, and the sum of three gamma random variables, respectively. [3, 6] However, these models are not always successful in fitting general MPEG frames. Figures 2-1 and 2-2 show the movie *Matrix Reloaded* B-frames histogram, pdf and

Table 2-1. B-frame errors of the movie *Matrix Reloaded*.

Probability Distributions	pdf errors [bytes]	cdf errors [bytes]
Rician	3.2762×10^{-11}	0.0017
Nakagami	3.6301×10^{-11}	0.0022
Gamma	4.1884×10^{-11}	0.0030
Weibull	5.7357×10^{-11}	0.0044
Lognormal	6.9409×10^{-11}	0.0070
Rayleigh	1.6511×10^{-10}	0.0307

Table 2-2. P-frame errors of the movie *Matrix Reloaded*.

Probability Distributions	pdf errors [bytes]	cdf errors [bytes]
Rician	2.9434×10^{-11}	0.0029
Nakagami	3.3355×10^{-11}	0.0037
Gamma	3.8642×10^{-11}	0.0051
Weibull	4.3932×10^{-11}	0.0054
Lognormal	6.0069×10^{-11}	0.0105
Rayleigh	1.1406×10^{-10}	0.0324

its empirical cdf, respectively. The six probability distributions are overlapped on the histogram and empirical cdfs of the B-frames in Figures 2-1 and 2-2. As we can see, the histogram of the movie *Matrix Reloaded* B-frames is more fitted to a single Rician distribution rather than a single Gamma distribution. We can also confirm this by the numerical results. Table 2-1 contains the *Matrix Reloaded* B-frame errors of each probability distribution measured by the MSE method. As a result of numerical evaluations, the best fitted model to the statistical model of the movie *Matrix Reloaded* B-frames is not a single Gamma distribution but a single Rician distribution. Figures from 2-3 to 2-6 show the statistical characteristics of other frame data (i.e. P-frames and I-frames). The best fitted models for the P-frames and I-frames are a single Rician distribution and a single Nakagami distribution, respectively. Tables 2-2 and 2-3 also support these results numerically. The statistical models for the movie *Matrix Reloaded* total frames in which B-frames, P-frames, and I-frames are merged together is shown

Table 2-3. I-frame errors of the movie *Matrix Reloaded*.

Probability Distributions	pdf errors [bytes]	cdf errors [bytes]
Rician	9.4135×10^{-12}	0.0025
Nakagami	8.9577×10^{-12}	0.0020
Gamma	9.1945×10^{-12}	0.0020
Weibull	1.5444×10^{-11}	0.0045
Lognormal	1.2100×10^{-11}	0.0029
Rayleigh	3.9521×10^{-11}	0.0198

Table 2-4. Total-frame errors of the movie *Matrix Reloaded*.

Probability Distributions	pdf errors [bytes]	cdf errors [bytes]
Lognormal	2.9391×10^{-11}	0.0017
Gamma	3.2055×10^{-11}	0.0020
Nakagami	4.0755×10^{-11}	0.0035
Weibull	4.8376×10^{-11}	0.0045
Rayleigh	5.7566×10^{-11}	0.0066
Rician	5.7566×10^{-11}	0.0066

in Figures 2-7 and 2-8. Apparently, a single Lognormal distribution is well fitted to the histogram of total frames. And numerical results in Table 2-4 support the results of these experiments. In Figure 2-7, the Rician distribution coincides with the Rayleigh distribution. The reason of this correspondence is the modified Bessel function which is appears in the Rician density function and its parameter. In general, when $\nu = 0$, the Rician distribution becomes the Rayleigh distribution. We can make sure of this relationship in Equations from (2–6) to (2–9). A general equation of the modified Bessel function of the first kind is

$$I_\nu(z) = \left(\frac{z}{2}\right)^\nu \sum_{k=0}^{\infty} \frac{\left(z^2/4\right)^k}{k!\,\Gamma(\nu+k+1)} \tag{2–8}$$

The order zero of the modified Bessel function of the first kind is

$$I_0\left(\frac{x\nu}{\sigma^2}\right) = \sum_{k=0}^{\infty} \frac{\left(z^2/4\right)^k}{\left(k!\right)^2}\Bigg|_{z=(x\nu)/\sigma^2} \tag{2–9}$$

Table 2-5. Estimated parameters for the movie *Matrix Reloaded* total frame.

Probability Distributions	Parameters	
Gamma	$k = 6.3285$	$\theta = 5.33 \times 10^3$
Lognormal	$\mu = 10.3457$	$\sigma = 0.4296$
Nakagami	$\mu = 1.6879$	$\omega = 1.34 \times 10^9$
Weibull	$\lambda = 3.79 \times 10^4$	$k = 2.4164$
Rician	$\nu = 64.0363$	$\sigma = 2.59 \times 10^4$
Rayleigh	$\sigma = 2.59 \times 10^4$	

If we consider Equation (2–7) and Equation (2–9) along with estimated parameters, we can obtain the result of the Rayleigh distribution. Finally, Table 2-5 shows the estimated parameters of the movie *Matrix Reloaded* total frames.

2.3 Results and Discussion

Chapter 2 proposes a single probability distribution as a statistical model of the MPEG-2 total frame size for multimedia traffic. Rigorous experiments has been conducted to figure out the best fitted single distribution model for the empirical MPEG-2 total frames which are extracted from the commercial DVD movie *Matrix Reloaded* and the evaluation for the total frames has been done by means of the MLE and MSE methods. The result of these experiments is such that the best fitted model for the statistical model of the MPEG-2 total frames turns out the Lognormal distribution. Moreover, extended applications to other DVD data also show the same results. But single distributions cannot explain the inherent multimodal property in the histogram of the movie *Matrix Reloaded*. Based on this result, it turns out that we need a more rigorous analysis on the statistical characteristics of MPEG multimedia traffic. This research will help the design of multimedia network systems.

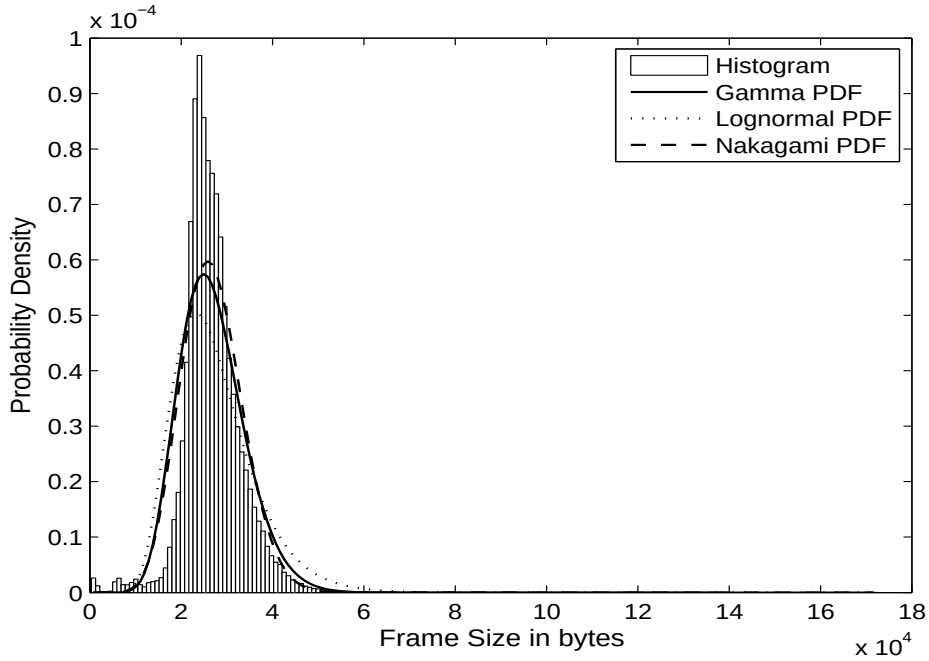

A Gamma distribution, Lognormal distribution, and Nakagami distribution

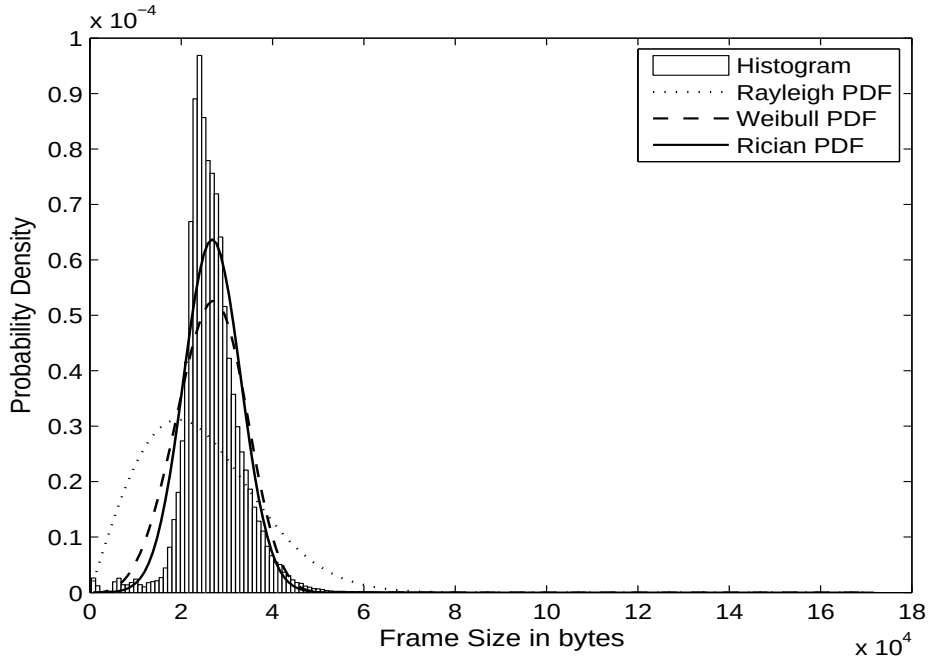

B Rayleigh distribution, Weibull distribution, and Rician distribution

Figure 2-1. Probability density functions of the movie *Matrix Reloaded* B-frame.

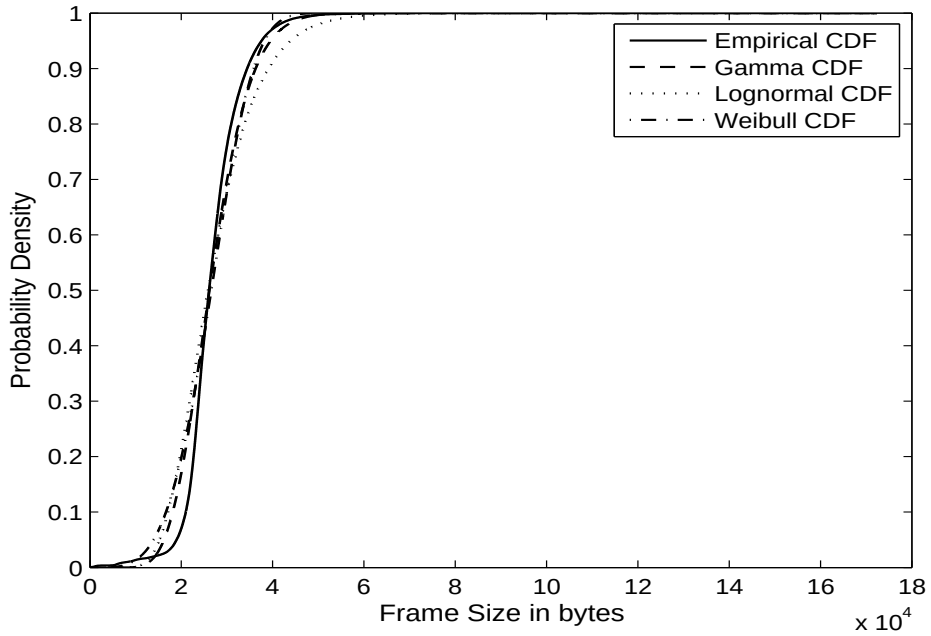

A Gamma distribution, Lognormal distribution, and Weibull distribution

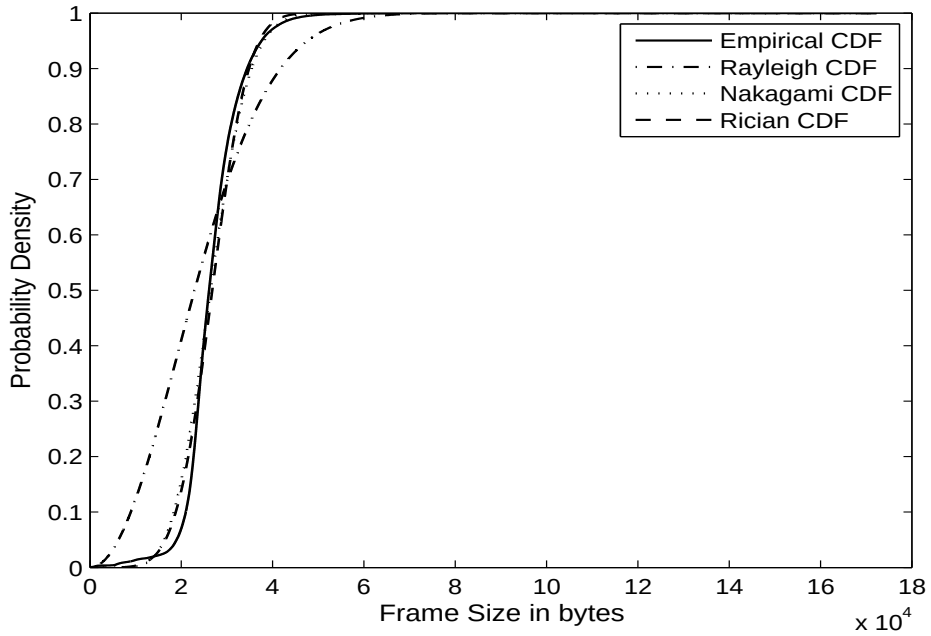

B Rayleigh distribution, Nakagami distribution, and Rician distribution

Figure 2-2. Cumulative distribution functions of the movie *Matrix Reloaded* B-frame.

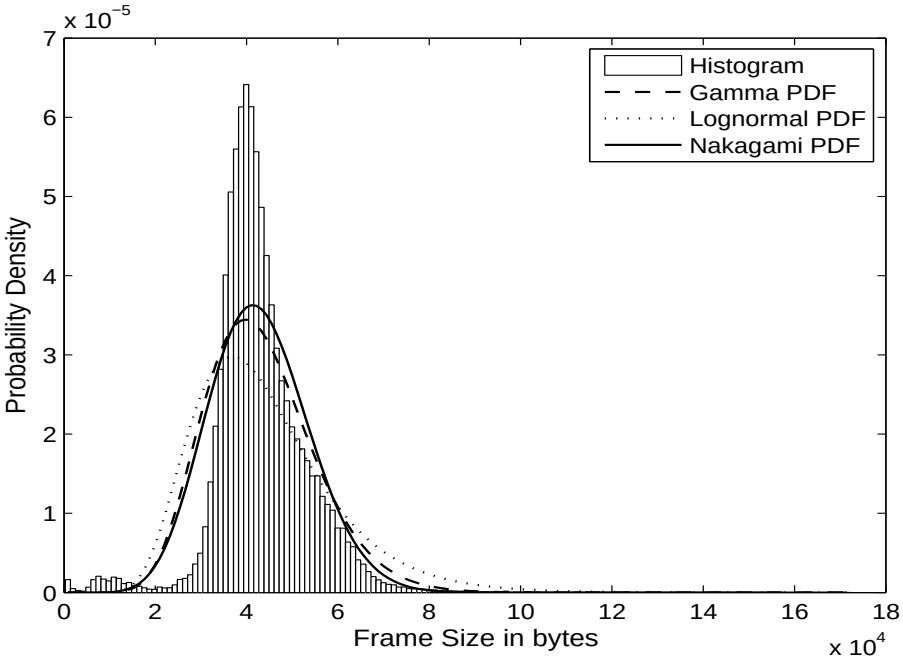

A Gamma distribution, Lognormal distribution, and Nakagami distribution

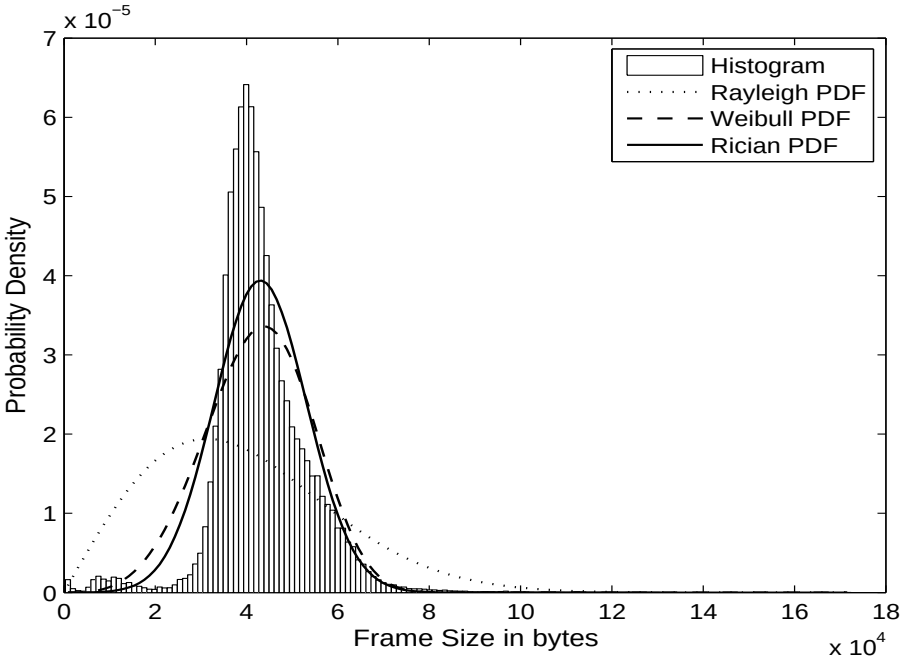

B Rayleigh distribution, Weibull distribution, and Rician distribution

Figure 2-3. Probability density functions of the movie *Matrix Reloaded* P-frame.

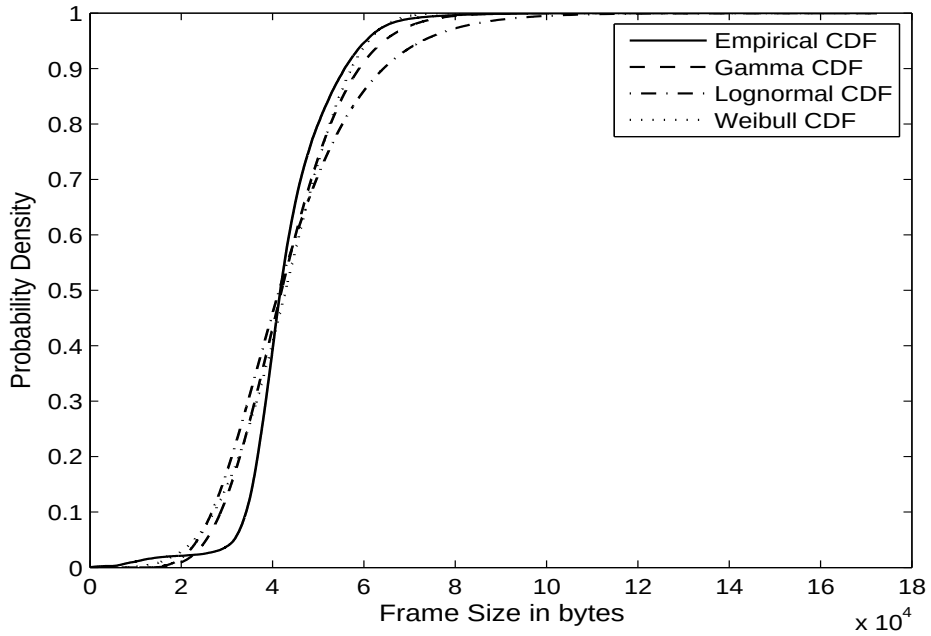

A Gamma distribution, Lognormal distribution, and Weibull distribution

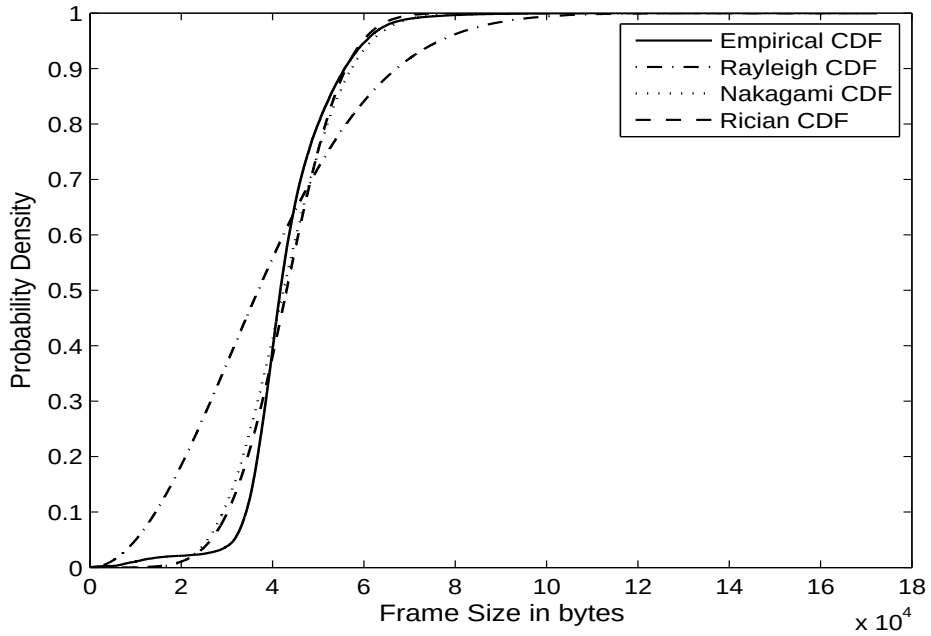

B Rayleigh distribution, Nakagami distribution, and Rician distribution

Figure 2-4. Cumulative distribution functions of the movie *Matrix Reloaded* P-frame.

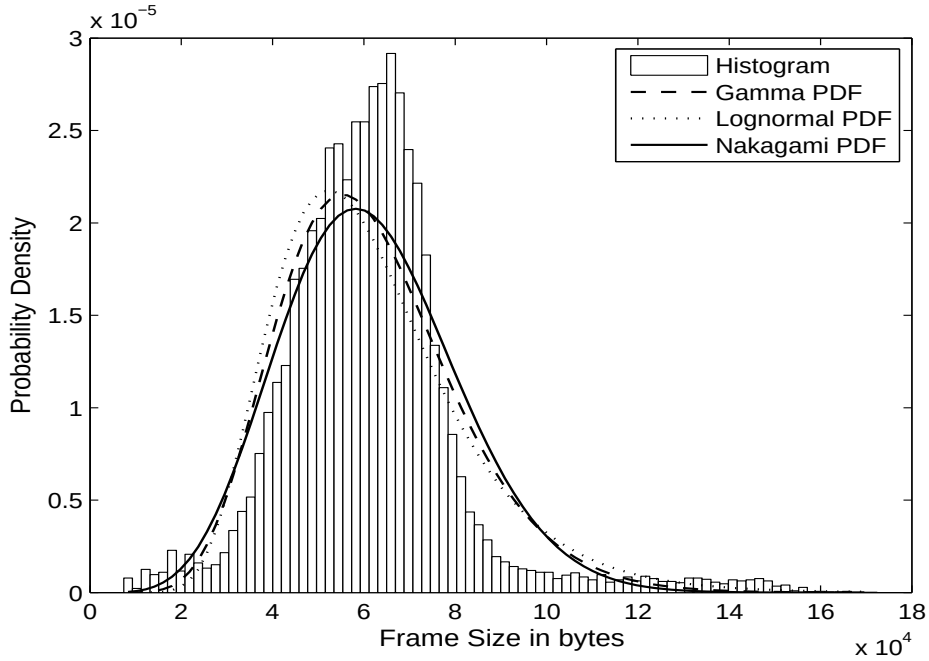

A Gamma distribution, Lognormal distribution, and Nakagami distribution

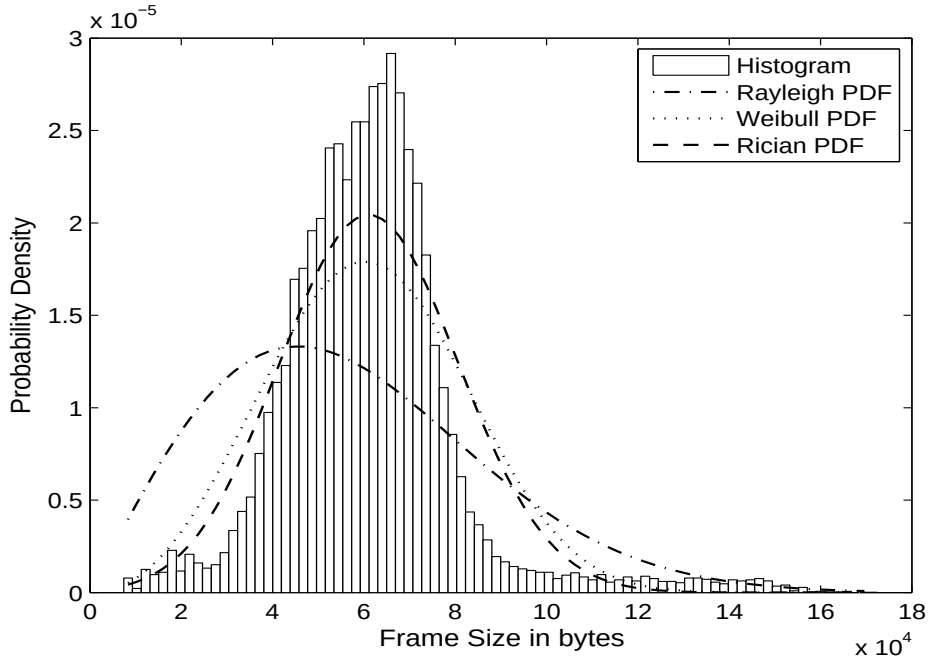

B Rayleigh distribution, Weibull distribution, and Rician distribution

Figure 2-5. Probability density functions of the movie *Matrix Reloaded* I-frame.

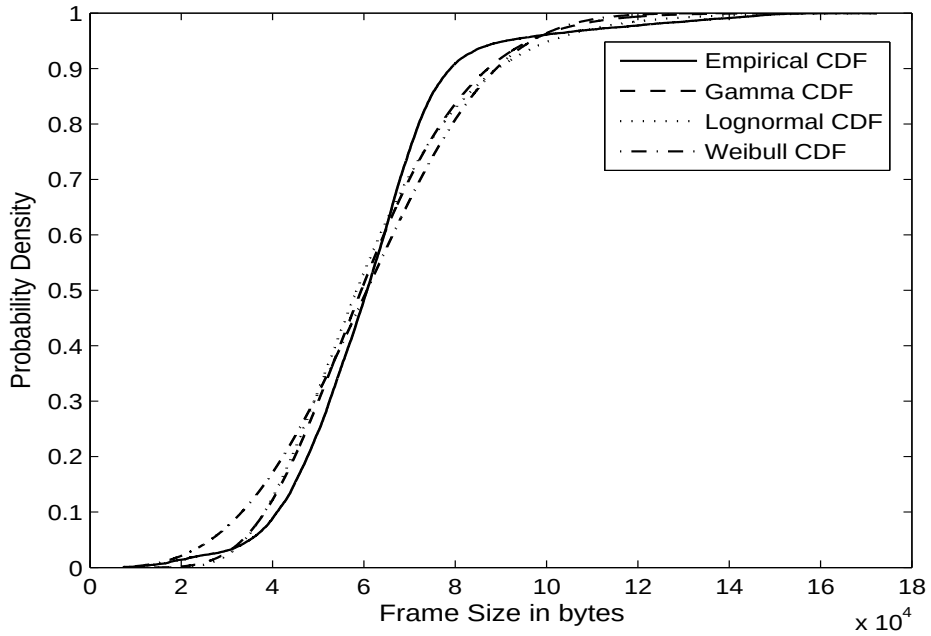

A Gamma distribution, Lognormal distribution, and Weibull distribution

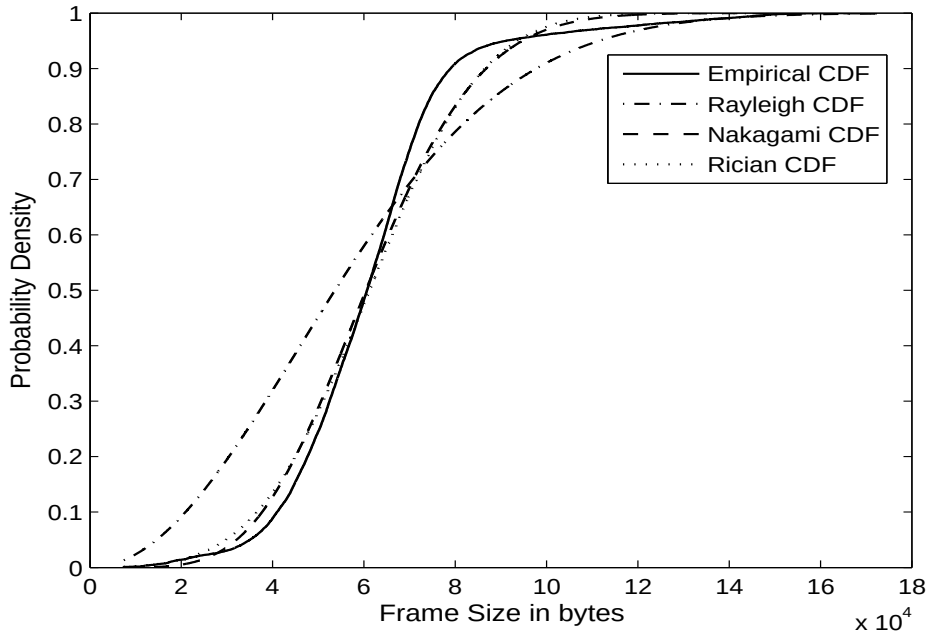

B Rayleigh distribution, Nakagami distribution, and Rician distribution

Figure 2-6. Cumulative distribution functions of the movie *Matrix Reloaded* I-frame.

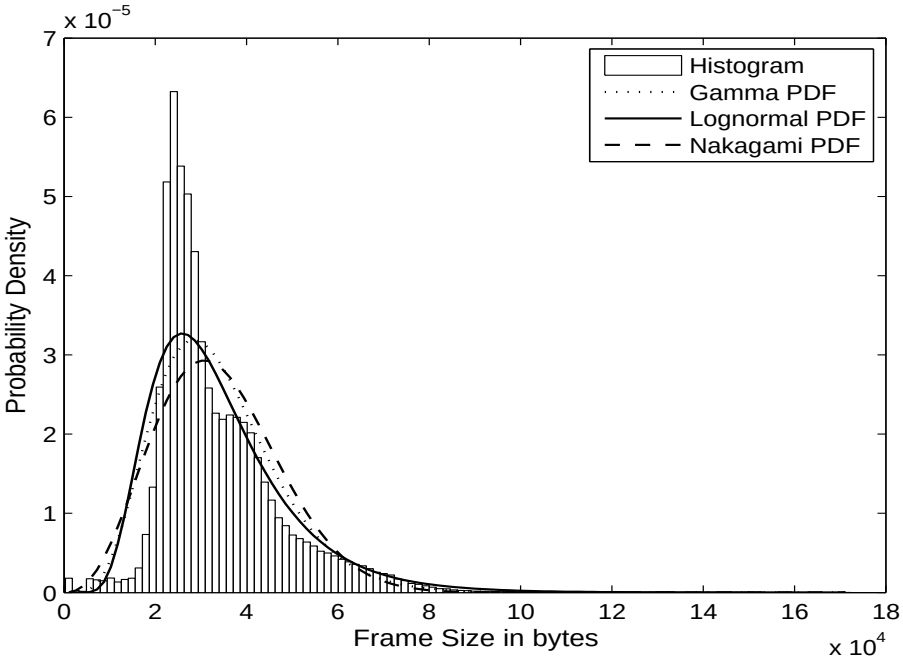

A Gamma distribution, Lognormal distribution, and Nakagami distribution

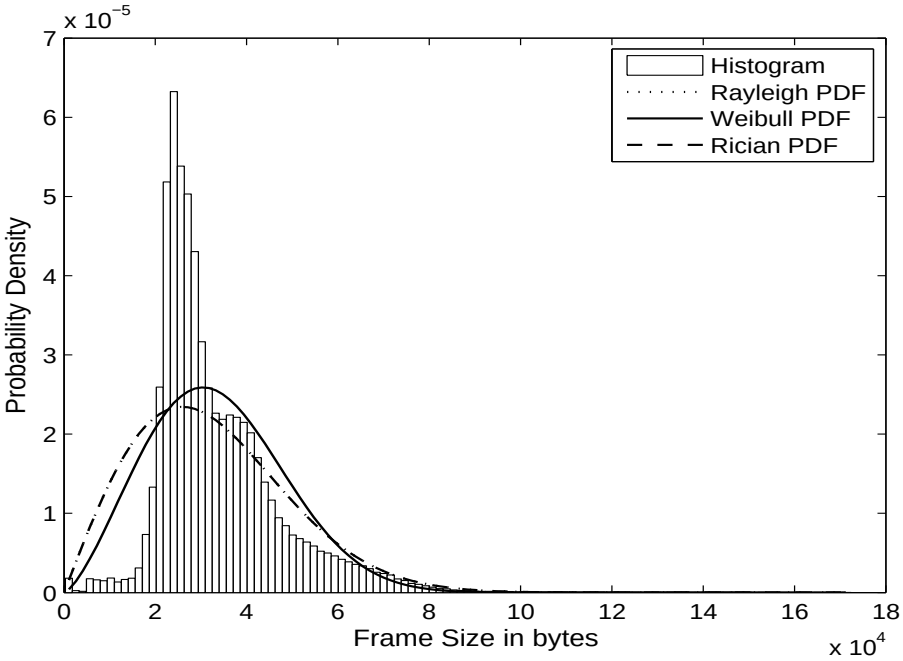

B Rayleigh distribution, Weibull distribution, and Rician distribution

Figure 2-7. Probability density functions of the movie *Matrix Reloaded* total frame.

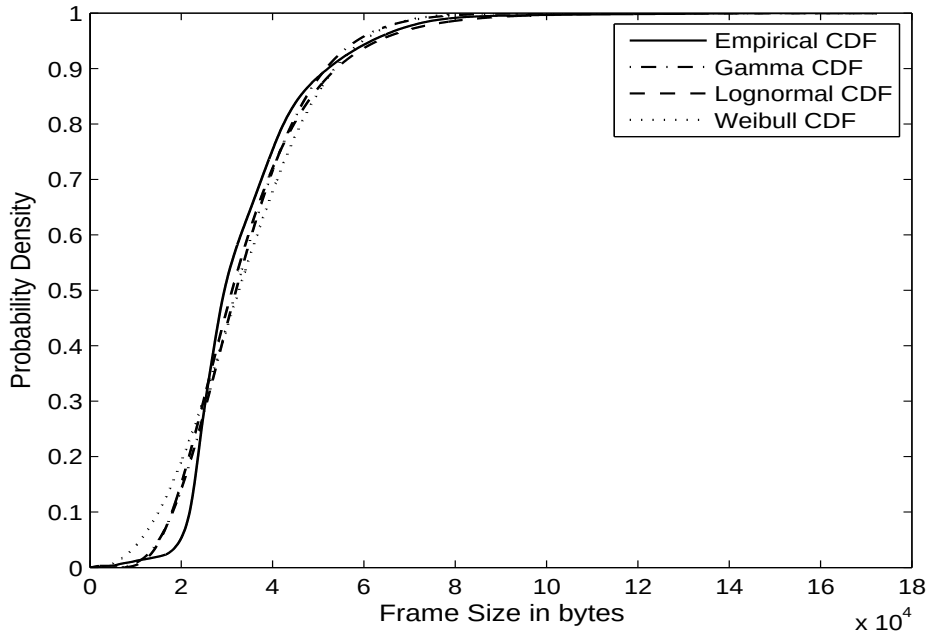

A Gamma distribution, Lognormal distribution, and Weibull distribution

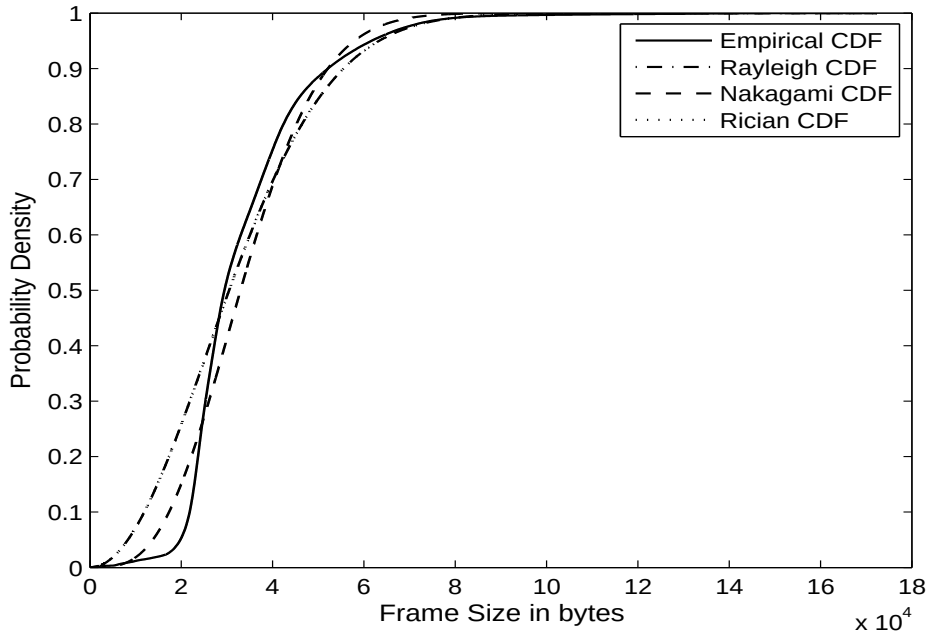

B Rayleigh distribution, Nakagami distribution, and Rician distribution

Figure 2-8. Cumulative distribution functions of the movie *Matrix Reloaded* total frame.

CHAPTER 3
STATISTICAL ANALYSIS OF MULTIMEDIA TRAFFIC OVER COMMUNICATION NETWORKS

3.1 An Overview of the Statistical Characteristics of Multimedia Traffic

Chapter 2 was devoted to the study of the statistical MPEG frame model with a single probability distribution; histograms for each of frame data and total frame data were fitted to single probability distributions. But, taking a careful look at the results from Chapter 2, we can realize that there are noticeable phenomena in the histograms. The fact is that the mode of the histogram is not unique and we can interpret these phenomena as a mixture of more than one unimodal distribution which has only one mode. When we start to analyze the mixture type of distributions, we need to make sure that the mixture type of distributions is different from a sum of independent random variables. The sum of random variables has a probability density function which is given by the convolution integral of each marginal density function, whereas the density function of the mixture type of distributions has a form of a weighted sum of each density function and weight coefficients should be in the range between zero and unity. An example of the sum of independent random variables is the k-Erlang distribution which is added up from single exponential random variable to k exponential random variables and an example of the mixture type density function is the Hyper-Exponential distribution which is introduced by Orlilk and Rappaport. [12]

Chapter 3 introduces a statistical model of the MPEG frames as the mixture type distribution, namely, the Hyper-Gamma distribution and presents an extensive analysis of its adequateness of the statistical model for multimedia traffic.

3.2 Hyper-Gamma Distribution

The Hyper-Gamma distribution is a generalized form of the Hyper-Exponential distribution which was introduced by Rappaport and Orlik [12], the Hyper-Erlang distribution which was introduced by Fang [10] and the Hyper-Chi-Square distribution. It is not abnormal that a Gamma distribution can be extended to many other probability

distributions by varying its parameter values. For example, if a shape parameter of a gamma density function is unity, then the Gamma distribution becomes an Exponential distribution. If the shape parameter is a positive integer k, then it becomes a sum of k independent, identically distributed exponential random variable, in other words, k-Erlang distribution. This versatility of the gamma random variable holds for the case of the Hyper-Gamma random variable. In the next section we define the Hyper-Gamma distribution and its properties.

3.2.1 Model Description

Let X be a Hyper-Gamma random variable. Note that the random variable X is not a sum of gamma random variables but a weighted sum of gamma density functions. As mentioned previously, the density function of a sum of random variables is represented by a convolution integral of the density function of each random variable. But, in this case, the density function of the Hyper-Gamma random variable can be represented as a weighted sum of the N different gamma density function, which is closed under convex combination; in other words, all coefficients for the density function of the Hyper-Gamma random variable are nonnegative and sum to unity. The density function of the Hyper-Gamma random variable is defined as

$$f_{hygam}(x) = \sum_{i=1}^{N} \alpha_i \frac{x^{k_i-1} e^{-\frac{x}{\theta_i}}}{{\theta_i}^{k_i} \Gamma(k_i)} \qquad x > 0 \tag{3–1}$$

where k_i is the ith element of a set of shape parameters **k** $= [k_1, k_2, k_3, \cdots, k_N]$ and θ_i is the ith element of a set of scale parameters $\boldsymbol{\theta}$ =$[\theta_1, \theta_2, \theta_3, \cdots, \theta_N]$. α_i is the ith element of a set of weights of each density function $\boldsymbol{\alpha}$ =$[\alpha_1, \alpha_2, \alpha_3, \cdots, \alpha_N]$ and sums to unity. Each parameter has a positive real value (i.e. $k_i > 0$, $\theta_i > 0$ and $0 \leq \alpha_i \leq 1$). In Equation (3–1), $\Gamma(k_i)$ is the gamma function defined by

$$\Gamma(k) = \int_0^\infty t^{k-1} e^{-t} dt \tag{3–2}$$

The distribution function of the Hyper-Gamma random variable can be expressed in terms of the lower incomplete gamma function.

$$\begin{aligned} F_{hygam}(x) &= \int_0^x \sum_{i=0}^{N} \alpha_i \frac{t^{k_i-1} e^{-\frac{t}{\theta_i}}}{\theta_i^{k_i} \Gamma(k_i)} dt \\ &= \sum_{i=1}^{N} \alpha_i \frac{\gamma(k_i, \frac{x}{\theta_i})}{\Gamma(k_i)} \end{aligned} \tag{3–3}$$

where the lower incomplete gamma function is defined as

$$\gamma(k, x) = \int_0^x t^{k-1} e^{-t} dt \tag{3–4}$$

We can specify the fundamental statistical characteristics of the Hyper-Gamma random variable by the concept of moment. In general, a density function of a random variable X can be completely described provided the expected values of all the powers of X are defined. The nth moment of the Hyper-Gamma random variable is given by

$$E_{hygam}(X^n) = (-1)^n \frac{d^n}{ds^n} F_{hygam}(s) \Big|_{s=0} \tag{3–5}$$

where $n = 1, 2, 3, \cdots$, and $F_{hygam}(s)$ is a Laplace transform of the Hyper-Gamma distribution and can be interpreted as another version of a characteristic function. The characteristic function and its Laplace transform of the Hyper-Gamma distribution is represented by

$$\begin{aligned} \Phi_{hygam}(w) &= \sum_{i=1}^{N} \alpha_i (1 - jw\theta_i)^{-k_i} \\ F_{hygam}(s) &= \sum_{i=1}^{N} \alpha_i (1 + \theta_i s)^{-k_i} \end{aligned} \tag{3–6}$$

Let $E_{hygam}(X)$ and $VAR_{hygam}(X)$ be the mean and variance of the Hyper-Gamma random variable. The expected value and variance of the Hyper-Gamma random variable can be expressed as the first moment and a difference of the second moment and the square of the first moment. We can obtain the first and second moments of the

Hyper-Gamma random variable from Equation (3–5).

$$E_{hygam}(X) = \sum_{i=1}^{N} \alpha_i k_i \theta_i \tag{3–7}$$

$$E_{hygam}(X^2) = \sum_{i=1}^{N} \alpha_i k_i (k_i + 1) {\theta_i}^2 \tag{3–8}$$

$$VAR_{hygam}(X) = \sum_{i=1}^{N} \alpha_i k_i (k_i + 1) {\theta_i}^2 - \left[\sum_{i=1}^{N} \alpha_i k_i \theta_i \right]^2 \tag{3–9}$$

3.2.2 The Family of the Hyper-Gamma Distributions

Some mixed-type random variables are special cases of the Hyper-Gamma random variable. An appropriate choice of the parameters k_i and θ_i of the Hyper-Gamma density function makes it possible to obtain another mixed-type of distributions. If we select and $k_i = 1$ and $\theta_i = 1/\mu_i$, then the Hyper-Gamma density function becomes the Hyper-Exponential density function which is proposed by Rappaport and Orlik. [12] The Hyper-Exponential density function can be specified by a weighted sum of N different exponential density functions. Each of them has μ_i which is a rate or scale parameter. α_i indicates a weight of the individual exponential density function and sums to the unity. Each parameter has a positive real value (i.e. $\mu_i > 0$ and $0 \leq \alpha_i \leq 1$). Let the density function, distribution function, mean and variance of the Hyper-Exponential random variable be $f_{hyex}(x)$, $F_{hyex}(x)$, $E_{hyex}(X)$, and $VAR_{hyex}(X)$, respectively.

$$\begin{aligned} f_{hyex}(x) &= \sum_{i=1}^{N} \alpha_i \left. \frac{x^{k_i - 1} e^{-\frac{x}{\theta_i}}}{\theta_i^{k_i} \Gamma(k_i)} \right|_{k_i = 1, \theta_i = \frac{1}{\mu_i}} \\ &= \sum_{i=1}^{N} \alpha_i \mu_i e^{-\mu_i x} \end{aligned} \tag{3–10}$$

$$F_{hyex}(x) = \sum_{i=1}^{N} \alpha_i (1 - e^{-\mu_i x}) \tag{3–11}$$

$$E_{hyex}(X) = \sum_{i=1}^{N} \frac{\alpha_i}{\mu_i} \tag{3–12}$$

$$E_{hyex}(X^2) = \sum_{i=1}^{N} \frac{2\alpha_i}{\mu_i^2} \tag{3–13}$$

$$VAR_{hyex}(X) = \left[\sum_{i=1}^{N} \frac{2\alpha_i}{\mu_i^2}\right] - \left(\sum_{i=1}^{N} \frac{\alpha_i}{\mu_i}\right)^2 \tag{3–14}$$

We can obtain the same result with the Hyper-Exponential distribution proposed by Rappaport and Orlik from Equation (3–10) to Equation (3–14). [12]

If we set $k_i = m_i$ and $\theta_i = 1/\lambda_i$, then the Hyper-Gamma density function becomes that of the Hyper-Erlang distribution which is proposed by Fang. [10] The density function of the Hyper-Erlang random variable is defined as a weighted sum of N different erlang density functions and has the following form:

$$\begin{aligned} f_{hyer}(x) &= \sum_{i=1}^{N} \alpha_i \frac{x^{k_i-1} e^{-\frac{x}{\theta_i}}}{\theta_i^{k_i}\Gamma(k_i)}\Bigg|_{k_i=m_i,\theta_i=\frac{1}{\lambda_i}} \\ &= \sum_{i=1}^{N} \alpha_i \frac{\lambda_i^{m_i} x^{m_i-1}}{(m_i-1)!} e^{-\lambda_i x} \end{aligned} \tag{3–15}$$

where $\Gamma(k_i) = (m_i - 1)!$ provided $k_i = m_i$ and m_i is a shape parameter and takes a nonnegative integer value for $i = 1, 2, \cdots, N$. λ_i is a scale parameter and has a positive real number. α_i has the same meaning as appeared in the Hyper-Exponential distribution. Equation (3–15) is identical to the Hyper-Erlang density function, if we select $\lambda_i = m_i\eta_i$ where m_i is defined by a nonnegative integer and η_i is positive number in [10]. The distribution function of the Hyper-Erlang random variable can be acquired from the integration of the density function.

$$\begin{aligned} F_{hyer}(x) &= \int_0^x \sum_{i=1}^{N} \alpha_i \frac{\lambda_i^{m_i} t^{m_i-1}}{(m_i-1)!} e^{-\lambda_i t} dt \\ &= \sum_{i=1}^{N} \alpha_i \frac{\gamma(m_i, \lambda_i x)}{(m_i-1)!} \end{aligned} \tag{3–16}$$

The first moment, the second moment and variance are given as follows:

$$E_{hyer}(X) = \sum_{i=1}^{N} \alpha_i \frac{m_i}{\lambda_i} \tag{3–17}$$

$$E_{hyer}(X^2) = \sum_{i=1}^{N} \alpha_i m_i(m_i+1)\frac{1}{\lambda_i^2} \tag{3–18}$$

$$VAR_{hyer}(X) = \sum_{i=1}^{N} \alpha_i \frac{m_i(m_i+1)}{\lambda_i^2} - \left[\sum_{i=1}^{N} \alpha_i \cdot \frac{m_i}{\lambda_i}\right]^2 \tag{3–19}$$

The Hyper-Chi-Square density function can be achieved from the Hyper-Gamma density function by setting the parameters and θ_i=2 and $k_i = \varphi_i/2$. The density function of the Hyper-Chi-Square random variable is also specified by a weighted sum of *N* different Chi-Square density functions and is given as follows:

$$\begin{aligned} f_{hycsq}(x) &= \sum_{i=1}^{N} \alpha_i \frac{x^{k_i-1}e^{-\frac{x}{\theta_i}}}{\theta_i^{k_i}\Gamma(k_i)}\Bigg|_{k_i=\frac{\varphi_i}{2},\theta_i=2} \\ &= \sum_{i=1}^{N} \alpha_i \frac{x^{\frac{\varphi_i}{2}-1}e^{-\frac{x}{2}}}{2^{\frac{\varphi_i}{2}}\Gamma\left(\frac{\varphi_i}{2}\right)} \end{aligned} \tag{3–20}$$

where φ_i is a positive integer and implies the number of degrees of freedom. α_i represents a weight of each Chi-Square density function and also sums to unity.

The distribution function of the Hyper-Chi-Square random variable can be obtained by integrating its density function.

$$F_{hycsq}(x) = \sum_{i=1}^{N} \alpha_i \frac{\gamma(\frac{\varphi_i}{2}, \frac{x}{2})}{\Gamma\left(\frac{\varphi_i}{2}\right)} \tag{3–21}$$

The first moment, the second moment and variance of the Hyper-Chi-Square random variable are given as follows:

$$E_{hycsq}(X) = \sum_{i=1}^{N} \alpha_i \varphi_i \tag{3–22}$$

$$E_{hycsq}(X^2) = \sum_{i=1}^{N} \alpha_i \varphi_i(\varphi_i+2) \tag{3–23}$$

$$VAR_{hycsq}(X) = \sum_{i=1}^{N} \alpha_i \varphi_i(\varphi_i+2) - \left(\sum_{i=1}^{N} \alpha_i \cdot \varphi_i\right)^2 \tag{3–24}$$

The Coefficient of Variation (CoV) that is a dimensionless value is one good way to measure statistical dispersion for a random variable. It is defined as the ratio of the

standard deviation to the mean. The CoV of the exponential distribution is always unity because the standard deviation of the exponential distribution is equal to its mean. In the case of the Hyper-Exponential distribution, the CoV is greater or equal to one, which means that the Hyper-Exponential distribution has greater dispersion than that of the exponential distribution. [12] The CoV of the Hyper-Erlang distribution can be adjustable to the desired value by changing the parameters; that is, it can have the value less than, equal to or greater than unity. [10] In case of the Hyper-Gamma distribution, the CoV is expressed by Equation (3–25).

$$CoV = \frac{\sqrt{\sum_{i=1}^{N} \alpha_i k_i (k_i + 1) {\theta_i}^2 - \left\{ \sum_{i=1}^{N} \alpha_i k_i \theta_i \right\}^2}}{\sum_{i=1}^{N} \alpha_i k_i \theta_i} \tag{3–25}$$

The CoV of the Hyper-Gamma distribution is always positive since the numerator (i.e. the standard deviation) and denominator (i.e. the first moment) of Equation (3–25) are positive. Basically, the first and second moments of the Hyper-Gamma distribution is always positive. If we take the square of CoV, then

$$CoV^2 = \frac{\sum_{i=1}^{N} \alpha_i k_i (k_i + 1) {\theta_i}^2 - \left\{ \sum_{i=1}^{N} \alpha_i k_i \theta_i \right\}^2}{\left\{ \sum_{i=1}^{N} \alpha_i k_i \theta_i \right\}^2} \tag{3–26}$$

If we look at the numerator of Equation (3–26) more closely, we can rewrite it as follows:

$$\left[\sum_{i=1}^{N} \alpha_i k_i^2 {\theta_i}^2 - \left\{ \sum_{i=1}^{N} \alpha_i k_i \theta_i \right\}^2 \right] + \sum_{i=1}^{N} \alpha_i k_i {\theta_i}^2 \tag{3–27}$$

Let Y be a discrete random variable which takes on values from a set $\{k_1\theta_1, k_2\theta_2, k_3\theta_3, \cdots, k_N\theta_N\}$ with probability α_1 in a similar way as appeared in [19]. Then the first and second terms in Equation (3–27) can be considered as the expected values of a random variable Y^2 and Y, thus the term in brackets in Equation (3–27) is considered as a variance of Y and

is always nonnegative. Moreover, the third term is obviously a positive and an increasing function.

3.3 Experimental Analysis

This section describes an experimental analysis of the MPEG-encoded commercial DVD movie frames and shows that an application of the results to empirical data provides an acceptable model for the characteristics of MPEG frame traffic. The methods used in this section to trace a stochastic model are empirical histograms and Bayesian Information Criterion (BICs) based on the maximum likelihood value of the MPEG frames which came from the famous commercial movie *Matrix* and *Lord of the Rings II*. To construct a probability histogram from raw frame data, the Freedman-Diaconis method is also selected as a decision rule of a bin size [18] as appeared in Equation (2–1). Moreover, for the purpose of the statistical identification, the BIC values are used [20]:

$$\text{BIC} = \xi ln(n) - 2ln(L) \tag{3–28}$$

where n is the same one used in Equation (2–1), ξ is the number of parameters in the stochastic model and L means the maximum likelihood value. Gamma, Lognormal, and Rayleigh distributions are presented to compare how well the Hyper-Gamma distribution is matched to the histograms of the empirical MPEG frames. Among the above competing distributions, the one which has the smallest BIC value is chosen as the best stochastic model for MPEG frames. Table 3-1 presents the mean, variance, and coefficient of variation for empirical data and the estimated Hyper-Gamma model, respectively, and one can make sure that there are no big difference in CoVs between empirical data and the estimated Hyper-Gamma model. Table 3-2 shows the BICs of three single distributions and we can recognize that the Gamma distribution has the smallest BICs for each frame of the two movies in single distribution case. Figures from 3-4 to 3-6 represent the statistical models of B-frames, P-frames, and I-frames

Table 3-1. Mean, variance and CoV of empirical data and the Hyper-Gamma distribution.

		B-frame	P-frame	I-frame
Matrix	Mean [1]	2.0104×10^4	3.4384×10^4	5.8147×10^4
Empirical	Variance	3.0337×10^7	7.8708×10^7	1.0255×10^8
Data	CoV	0.2740	0.2580	0.1742
Hyper	Mean	2.0104×10^4	3.4384×10^4	5.8147×10^4
Gamma	Variance	3.0625×10^7	8.0376×10^7	1.0336×10^8
Distribution	CoV	0.2753	0.2607	0.1748
LoRII	Mean	2.0395×10^4	3.9655×10^4	7.2200×10^4
Empirical	Variance	1.0070×10^8	2.7822×10^8	7.4036×10^8
Data	CoV	0.4920	0.4206	0.3769
Hyper	Mean	2.0395×10^4	3.9655×10^4	7.2200×10^4
Gamma	Variance	1.0100×10^8	2.8310×10^8	7.3988×10^8
Distribution	CoV	0.4928	0.4243	0.3767

[1] Units of mean and variance are measured in bytes.

Table 3-2. The BICs of three single distributions.

Single	*Matrix*		
Distributions	B-frame	P-frame	I-frame
Gamma	2614464.11	1027206.43	351689.94
Lognormal	2620012.01	1032887.05	354794.79
Rayleigh	2702306.10	1061707.03	370863.32
Single	*Lord of the Rings II*		
Distributions	B-frame	P-frame	I-frame
Gamma	3636977.49	1443017.99	498437.14
Lognormal	3660244.09	1461541.60	499906.72
Rayleigh	3639226.32	1443057.18	503278.33

of the movie *Matrix*, and Figures from 3-7 to 3-9 are for the movie *Lord of the Rings II*, respectively.

When we examine histograms of the frames from two movies, *Matrix* and *Lord of the Rings II*, we can recognize that similar situation arises. If we take a glance at them,

Table 3-3. The BICs of the Hyper-Gamma distribution for the two movies.

	Matrix			*LoR II*		
♯[2]	B-frame	P-frame	I-frame	B-frame	P-frame	I-frame
1	2614464	1027206	351689	3636977	1443018	498437
2	2602588	1023160	346959	3629093	1434713	497491
3	2602209	1022772	346936	3619361	1433275	496522
4	2601956	1022696	346952	3617879	1433199	496293
5	2601662	1022250	346927	3617844	1433108	496321
6	2601379	1022246	346897	3617846	1433086	496335
7	2601120	1022258	346902	3617885	1433113	496138
8	2601070	1022286	346921	3617931	1433128	496160
9	2600770	1022320	346947	3617979	1433141	496176
10	2600756	1022363	346979	3618002	1433149	496142
11	2600665	1022403	347000	3618041	1433172	496168
12	2600653	1022425	347027	3618048	1433210	496198
13	2600662	1022450	347059	3618084	1433239	496214
14	2600679	1022479	347082	3618110	1433278	496240
15	2600718	1022506	347073	3618140	1433309	496241
16	2600726	1022537	347093	3618139	1433344	496287
17	2600730	1022568	347124	3618147	1433375	496301
18	2600758	1022606	347147	3618182	1433410	496324
19	2600777	1022640	347172	3618215	1433445	496353
20	2600822	1022670	347198	3618248	1433464	496378
21	2600826	1022702	347213	3618262	1433492	496408
22	2600862	1022731	347241	3618298	1433512	496436
23	2600893	1022765	347271	3618309	1433543	496472
24	2600911	1022664	347294	3618369	1433567	496502
25	2600950	1022824	347322	3618374	1433582	496518
26	2601003	1022858	347344	3618405	1433618	496560
27	2601020	1022888	347375	3618426	1433645	496579
28	2601044	1022781	347395	3618476	1433665	496612
29	2601079	1022812	347426	3618496	1433702	496642
30	2601105	1022843	347448	3618526	1433723	496668

[2] The ♯ symbol implies the number of clusters.

we can easily find out that histograms of the movie *Matrix* show a unimodal property, whereas the *Lord of the Rings II* histograms have a multimodal property. The unimodal distribution has only one maximum value at its mode and no other local maxima; thus

its histogram may be approximated by a unimodal function, a single probability density function in this case. But the density function of each frame of the movie *Matrix* is not composed of a single probability distribution. We can make sure of this from BIC values in Table 3-3 showing the number of clusters which is referred to as the component distribution of the Hyper-Gamma distribution and also confirm this from Subfigures A's in Figures from 3-1 to 3-3. We can identify the smallest BICs of each frame in Table 3-3 and it means that the proper stochastic model for each frame of the movie *Matrix* is not a single distribution but several or more numbers of component distributions are synthesized. Meanwhile, the multimodal distribution has M $(M = 2, 3, 4, \cdots)$ distinct local maximums at their modes in its density function. The *Lord of the Rings II* histogram cannot be explained with a unimodal distribution but can be approximated by a multimodal distribution with M different modes because there are more than one local maximum in its histogram. We can also make sure of this from BIC values in Table 3-3 and Subfigures B's in Figures from 3-1 to 3-3. Consequently, they can be interpreted as a mixed type of a number of different probability distributions. The following steps are conducted to figure out how many different distributions are composed of the frame data.

Step1 Perform a conventional K-means clustering based on Euclidean distance with raw frame data.

Step2 Estimate the parameters (i.e. weight, shape and scale parameters) of each cluster by means of the Maximum Likelihood Estimation.

Step3 Recompose the clusters of raw frame data based on a posteriori probability with each parameter which is obtained in the step 2.

Step4 Estimate the parameters (i.e. weight, shape and scale parameters) of raw frame data by means of the Expectation Maximization algorithm with the initial values obtained from the step 2.

Table 3-4. Parameters of each component of the Hyper-Gamma distribution for the movie *Matrix*.

Frames	Weight	Shape	Scale
B Frame	$\alpha_1 = 0.0449$	$k_1 = 2.8447 \times 10^2$	$\theta_1 = 9.7159 \times 10^1$
	$\alpha_2 = 0.0324$	$k_2 = 3.0069 \times 10^1$	$\theta_2 = 1.1090 \times 10^3$
	$\alpha_3 = 0.1181$	$k_3 = 1.2489 \times 10^2$	$\theta_3 = 1.2578 \times 10^2$
	$\alpha_4 = 0.1260$	$k_4 = 8.0240 \times 10^2$	$\theta_4 = 2.4785 \times 10^1$
	$\alpha_5 = 0.0785$	$k_5 = 5.5956 \times 10^2$	$\theta_5 = 4.1127 \times 10^1$
	$\alpha_6 = 0.1198$	$k_6 = 4.0094 \times 10^2$	$\theta_6 = 4.2977 \times 10^1$
	$\alpha_7 = 0.1100$	$k_7 = 7.1188 \times 10^2$	$\theta_7 = 2.9990 \times 10^1$
	$\alpha_8 = 0.1220$	$k_8 = 6.9031 \times 10^2$	$\theta_8 = 2.6883 \times 10^1$
	$\alpha_9 = 0.0456$	$k_9 = 1.2461 \times 10^2$	$\theta_9 = 2.4892 \times 10^2$
	$\alpha_{10} = 0.0069$	$k_{10} = 1.2450 \times 10^0$	$\theta_{10} = 1.6187 \times 10^4$
	$\alpha_{11} = 0.0581$	$k_{11} = 4.2666 \times 10^2$	$\theta_{11} = 5.8772 \times 10^1$
	$\alpha_{12} = 0.1377$	$k_{12} = 1.9336 \times 10^1$	$\theta_{12} = 7.2399 \times 10^2$
P Frame	$\alpha_1 = 0.2892$	$k_1 = 2.6361 \times 10^1$	$\theta_1 = 1.0398 \times 10^3$
	$\alpha_2 = 0.1545$	$k_2 = 1.1712 \times 10^2$	$\theta_2 = 3.1424 \times 10^2$
	$\alpha_3 = 0.2868$	$k_3 = 1.1598 \times 10^2$	$\theta_3 = 2.7177 \times 10^2$
	$\alpha_4 = 0.0176$	$k_4 = 1.5583 \times 10^0$	$\theta_4 = 1.9938 \times 10^4$
	$\alpha_5 = 0.1464$	$k_5 = 6.9652 \times 10^1$	$\theta_5 = 6.1789 \times 10^2$
	$\alpha_6 = 0.1056$	$k_6 = 2.3361 \times 10^1$	$\theta_6 = 1.9811 \times 10^3$
I Frame	$\alpha_1 = 0.1728$	$k_1 = 2.8738 \times 10^1$	$\theta_1 = 1.7654 \times 10^3$
	$\alpha_2 = 0.0210$	$k_2 = 2.3421 \times 10^0$	$\theta_2 = 1.5161 \times 10^4$
	$\alpha_3 = 0.1252$	$k_3 = 4.0722 \times 10^1$	$\theta_3 = 1.6469 \times 10^3$
	$\alpha_4 = 0.1969$	$k_4 = 2.8511 \times 10^2$	$\theta_4 = 2.0576 \times 10^2$
	$\alpha_5 = 0.2374$	$k_5 = 1.9459 \times 10^2$	$\theta_5 = 3.3791 \times 10^2$
	$\alpha_6 = 0.2468$	$k_6 = 1.5019 \times 10^2$	$\theta_6 = 3.5298 \times 10^2$

Step5 Reshape the clusters of raw frame data with a posteriori probability based on the parameters obtained from the step 4.

Step6 Compare the BICs of each partitioned data obtained from the step 5 with the parameters obtained from the step 4.

Table 3-5. Parameters of each component of the Hyper-Gamma distribution for the movie *Lord of the Rings II*.

Frames	Weight	Shape	Scale
B Frame	$\alpha_1 = 0.1607$	$k_1 = 6.8726 \times 10^1$	$\theta_1 = 5.4250 \times 10^2$
	$\alpha_2 = 0.1366$	$k_2 = 4.8606 \times 10^1$	$\theta_2 = 5.5488 \times 10^2$
	$\alpha_3 = 0.4387$	$k_3 = 1.2370 \times 10^1$	$\theta_3 = 1.0834 \times 10^3$
	$\alpha_4 = 0.1967$	$k_4 = 2.9105 \times 10^1$	$\theta_4 = 6.8420 \times 10^2$
	$\alpha_5 = 0.0673$	$k_5 = 1.2173 \times 10^0$	$\theta_5 = 1.1260 \times 10^4$
P Frame	$\alpha_1 = 0.0583$	$k_1 = 0.8543 \times 10^0$	$\theta_1 = 3.4200 \times 10^4$
	$\alpha_2 = 0.0876$	$k_2 = 1.7300 \times 10^1$	$\theta_2 = 3.4989 \times 10^3$
	$\alpha_3 = 0.1592$	$k_3 = 3.7915 \times 10^1$	$\theta_3 = 9.7121 \times 10^2$
	$\alpha_4 = 0.1841$	$k_4 = 6.6817 \times 10^1$	$\theta_4 = 8.5301 \times 10^2$
	$\alpha_5 = 0.3519$	$k_5 = 1.3469 \times 10^1$	$\theta_5 = 1.9415 \times 10^3$
	$\alpha_6 = 0.1588$	$k_6 = 7.1164 \times 10^1$	$\theta_6 = 6.2715 \times 10^2$
I Frame	$\alpha_1 = 0.1044$	$k_1 = 1.0317 \times 10^2$	$\theta_1 = 9.1870 \times 10^2$
	$\alpha_2 = 0.3695$	$k_2 = 2.4767 \times 10^1$	$\theta_2 = 2.1557 \times 10^3$
	$\alpha_3 = 0.1737$	$k_3 = 1.2728 \times 10^2$	$\theta_3 = 6.3883 \times 10^2$
	$\alpha_4 = 0.0407$	$k_4 = 2.7007 \times 10^0$	$\theta_4 = 1.1929 \times 10^4$
	$\alpha_5 = 0.2017$	$k_5 = 5.7582 \times 10^1$	$\theta_5 = 1.1215 \times 10^3$
	$\alpha_6 = 0.0914$	$k_6 = 1.0473 \times 10^2$	$\theta_6 = 1.1782 \times 10^3$
	$\alpha_7 = 0.0186$	$k_7 = 8.2096 \times 10^2$	$\theta_7 = 1.8589 \times 10^2$

The method of determining the number of clusters described in the above is originated from the X-means algorithm. [21] Pelleg and Moore introduced one way of how to choose the number of clusters in given data; they applied a conventional K-means method and Bayesian Information Criterion (BIC) to given data. The conventional K-means method is undoubtedly one of the well-known clustering algorithm but it still has some misclassified data in its results. To reduce the number of misclassified data, two more repartition steps in which is described in step 3 and step 5 are added; a decision rule of members of each cluster is to choose the cluster which has the maximum value of a posteriori probability. We can generalize this by the followings; We are already given a set of raw frame data, $X = \{x_1, x_2, \cdots, x_j, \cdots, x_n\}$, n is the

total number of samples in raw data and the arbitrary number of clusters, $C = \{c_i\}$, $i \in \{1, 2, \cdots, N, \cdots\}$ from the result of the conventional K-means clustering, where N is the total number of clusters of which raw frame data are composed. Moreover we want to know the cluster in which each element x_j of X belongs. One of the most likely cases for us to do is to choose the cluster which has the biggest posteriori probability $p[C|X]$. The Hyper-Gamma distribution is already defined in Equation (3–1) and its posteriori probability is given by

$$f(x|W) = \sum_{i=1}^{N} \alpha_i p(x|\Phi_i) = \sum_{i=1}^{N} \alpha_i \frac{x^{k_i-1} e^{-\frac{x}{\theta_i}}}{\theta_i^{k_i} \Gamma(k_i)} \tag{3–29}$$

where α_i denotes a probability (i.e. weight) of the ith component density function $p(x|\Phi_i)$, Φ_i denotes a parameter vector fully specifying the ith component density function $p(x|\Phi_i)$, and W denotes a set of all parameters fully specifying the Hyper-Gamma density function $f(x|W)$, where $W = \{w_i\}$, $w_i = \{\alpha_i, \Phi_i\}$, $\Phi_i = \{k_i, \theta_i\}$, and $i \in \{1, 2, \cdots, N\}$. When we consider the simple case of two clusters C_1 and C_2, x_j belongs to C_1 if $p[C_1|x_j] > p[C_2|x_j]$, otherwise x_j belongs to C_2. Here we apply the Bayes' theorem, we can obtain the followings:

$$\begin{aligned} x_j \in C_1 \quad &\text{if} \quad \frac{p(x_j|\Phi_1)\alpha_1}{p(x_j)} > \frac{p(x_j|\Phi_2)\alpha_2}{p(x_j)} \\ x_j \in C_2 \quad &\text{if} \quad \frac{p(x_j|\Phi_1)\alpha_1}{p(x_j)} < \frac{p(x_j|\Phi_2)\alpha_2}{p(x_j)} \end{aligned} \tag{3–30}$$

Therefore, we can determine the cluster in which x_j belongs by means of

$$\begin{aligned} x_j \in C_1 \quad &\text{if} \quad p(x_j|\Phi_1)\alpha_1 > p(x_j|\Phi_2)\alpha_2 \\ x_j \in C_2 \quad &\text{if} \quad p(x_j|\Phi_1)\alpha_1 < p(x_j|\Phi_2)\alpha_2 \end{aligned} \tag{3–31}$$

In general,

$$\widehat{C}_i = \arg\max_i \quad \alpha_i p(x_j|\Phi_i) \tag{3–32}$$

$\widehat{C}_i$ represents the cluster in which x_j belongs, where i and j are integers and $j \leq n$. After gathering cluster information, we can obtain all parameters for each component of the Hyper-Gamma distribution through the step 2 to the step 5. Table 3-4 and Table 3-5 show the estimated parameters of each frame of the two movies. The one which has the smallest BIC is chosen as the best fitted model for a stochastic model of two movie frames and determine how many different distributions consist in each frame of two movies. The stochastic models for B-frames, P-frames, and I-frames of the movie *Matrix* and *Lord of the Rings II* can be approximated by the Hyper-Gamma distribution composed of a sum of 12, 6, and 6 different gamma density functions and a sum of 5, 6, and 7 different gamma density functions, respectively. The histograms of each frame of the two movies, the density functions of three single distributions, the density functions of the Hyper-Gamma distributions and their individual components are given in Figures from 3-4 to 3-9. Finally, based on these results, all single probability distributions represent poor performance than that of the Hyper-Gamma distribution. Thus it turns out that the best fitted models for each frame of the two movies are not single probability distributions, but rather the Hyper-Gamma distributions.

3.4 Results and Discusstion

MPEG video traffic modeling is an important issue for a design of network systems based on multimedia traffic since the massiveness of data can cause high transmission delay and low QoS. To resolve this problem, we need to estimate an accurate model for multimedia traffic. Chapter 3 proposes a stochastic model for multimedia traffic, the Hyper-Gamma distribution which is a generalized form of the Hyper-Exponential distribution, Hyper-Erlang distribution, and Hyper-Chi-square distribution. The multimedia traffic models proposed in the previous literature cannot explain the inherent multimodality in MPEG-2 frame data, whereas the Hyper-Gamma distribution model is able to predict the statistical characteristics of multimedia traffic over communication channels. The result of this studies establishes that the Hyper-Gamma distribution

model enables the construction of a stochastic model for multimedia traffic based on MPEG-2 frame data. Moreover, we can predict throughput and transmission delay of multimedia traffic from the estimated Hyper-Gamma distribution and this is helpful when we try to design a network system.

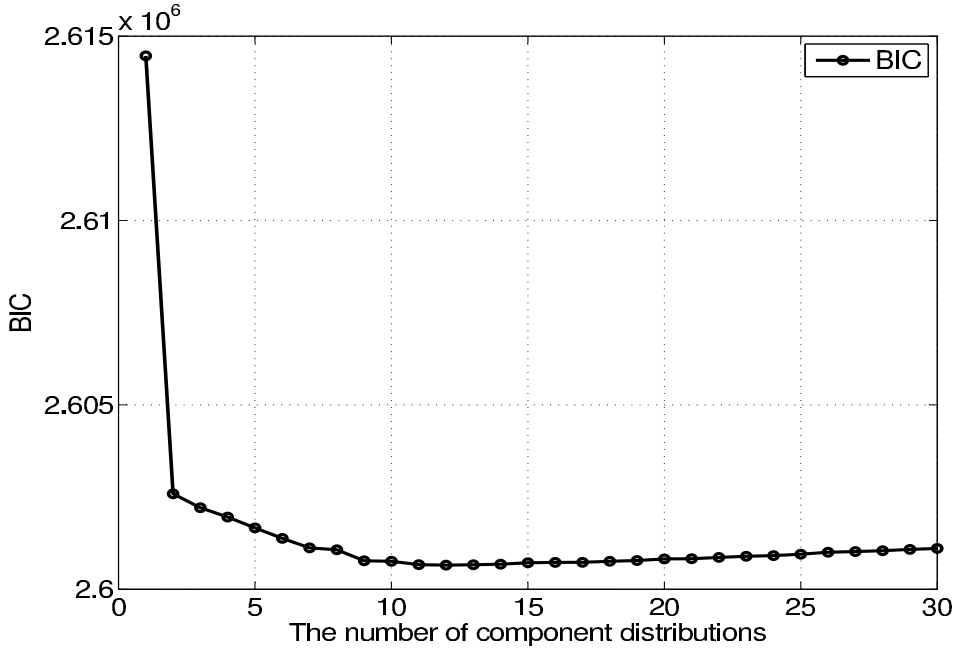

A The movie *Matrix*

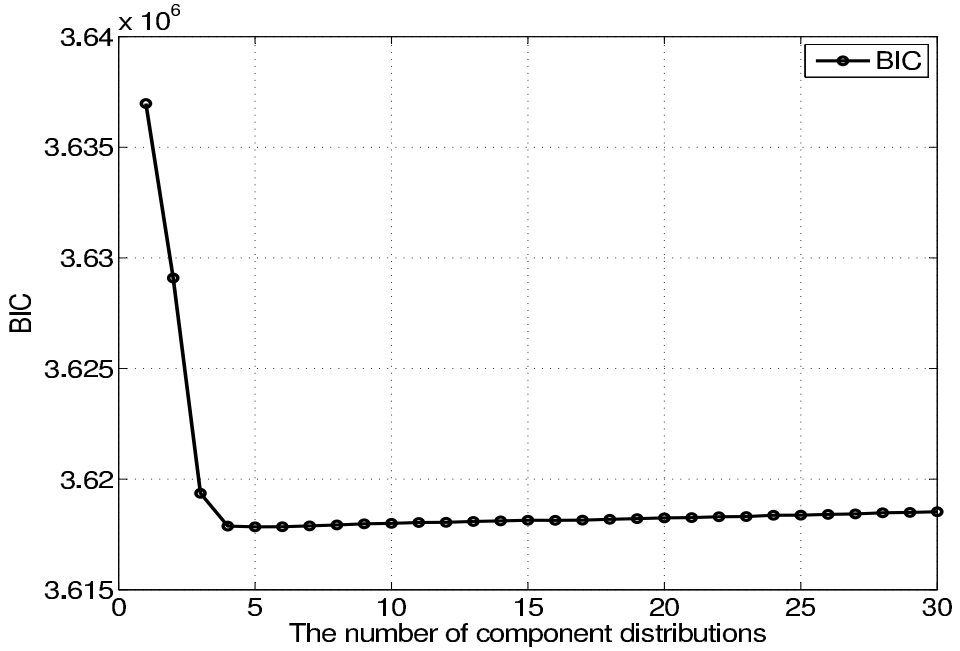

B The movie *Lord of the Rings II*

Figure 3-1. BIC values for each component distributions of the B-frames of the movie *Matrix* and *Lord of the Rings II*.

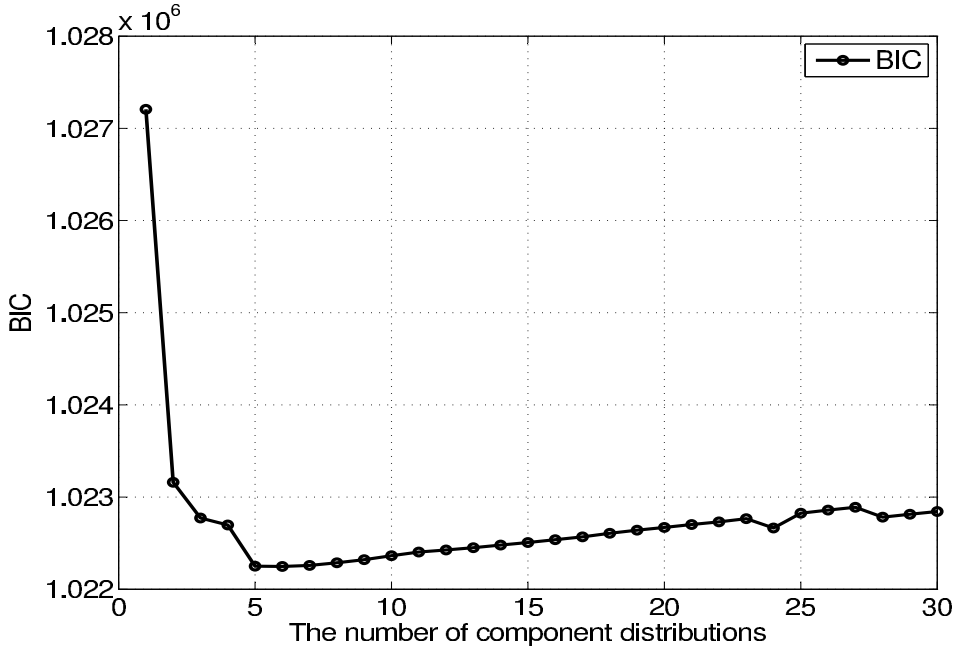

A The movie *Matrix*

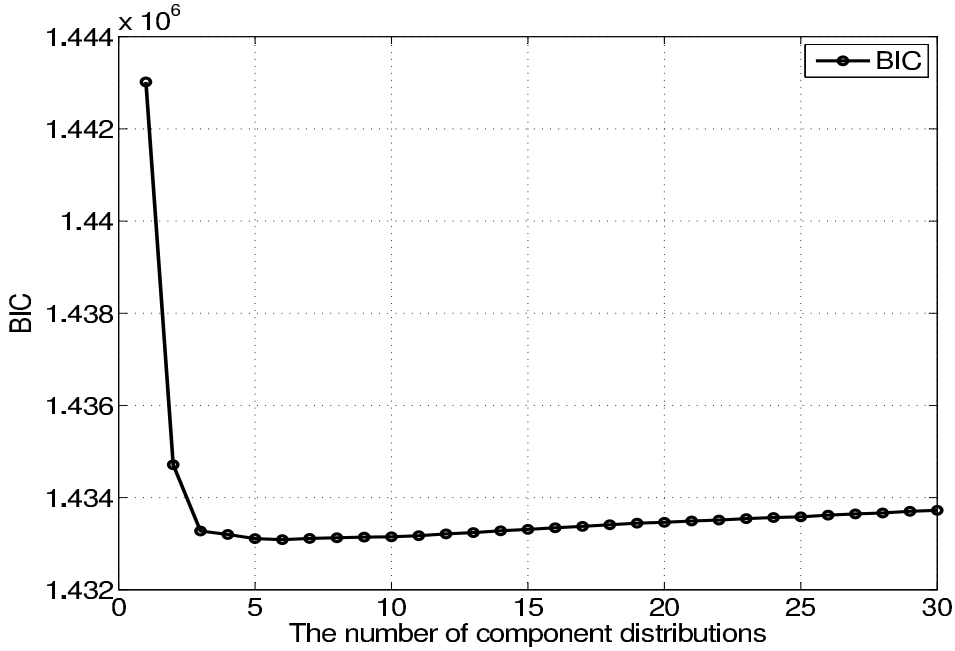

B The movie *Lord of the Rings II*

Figure 3-2. BIC values for each component distributions of the P-frames of the movie *Matrix* and *Lord of the Rings II*.

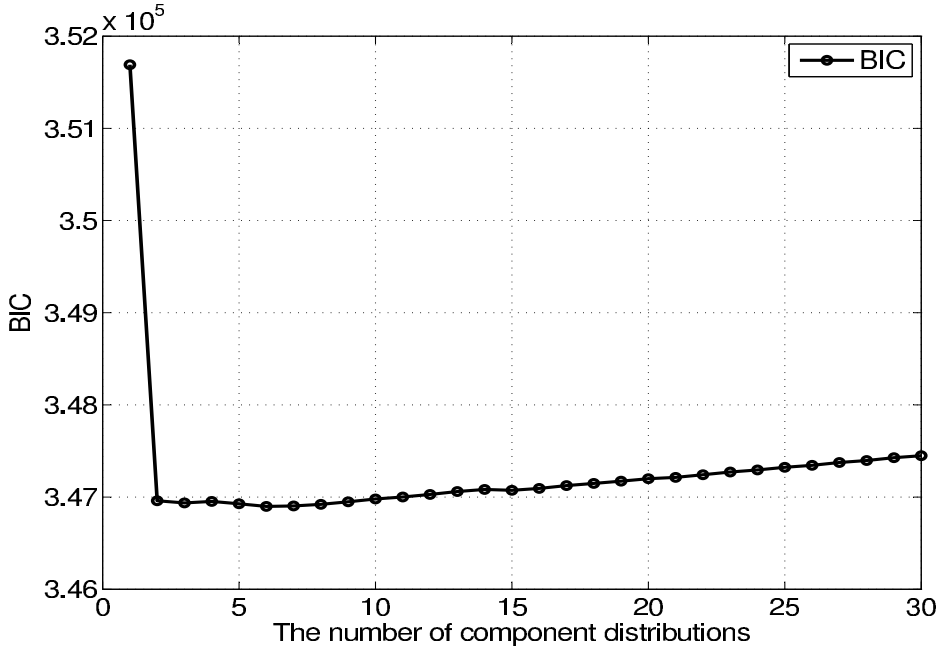

A The movie *Matrix*

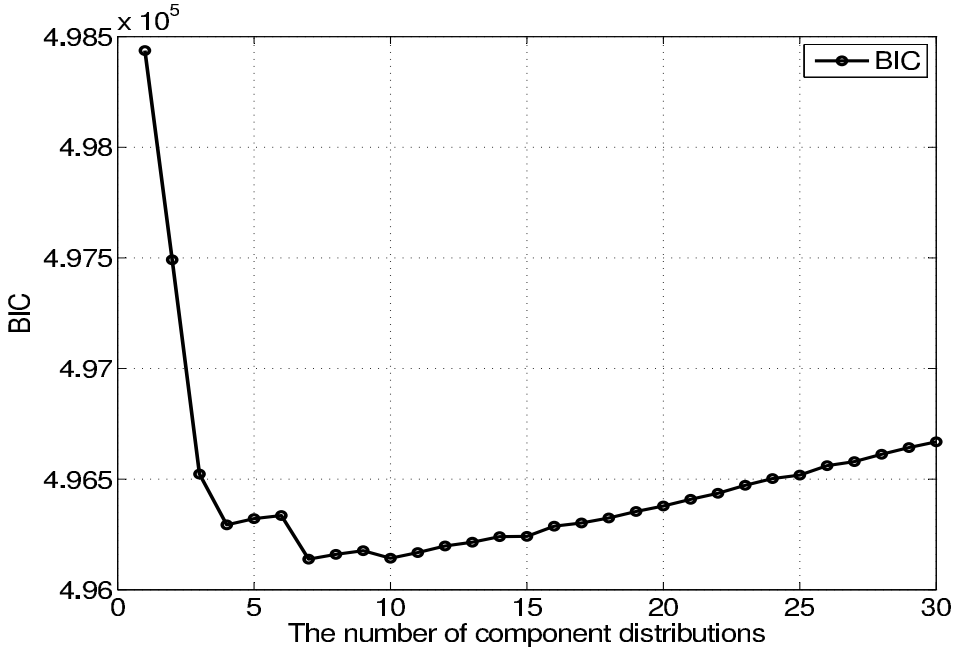

B The movie *Lord of the Rings II*

Figure 3-3. BIC values for each component distributions of the I-frames of the movie *Matrix* and *Lord of the Rings II*.

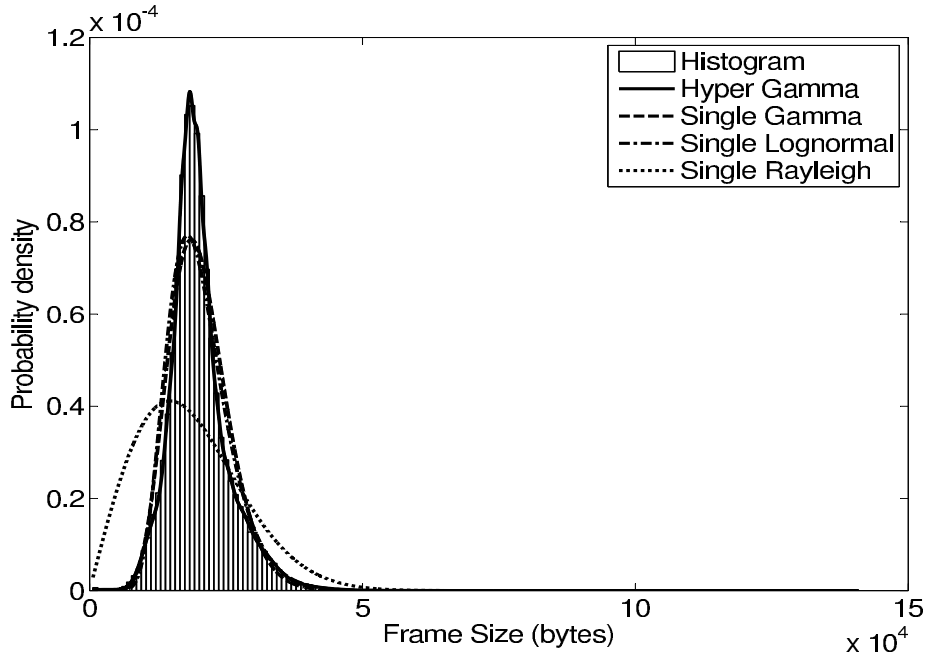

A Histogram, single density functions, and Hyper-Gamma density function

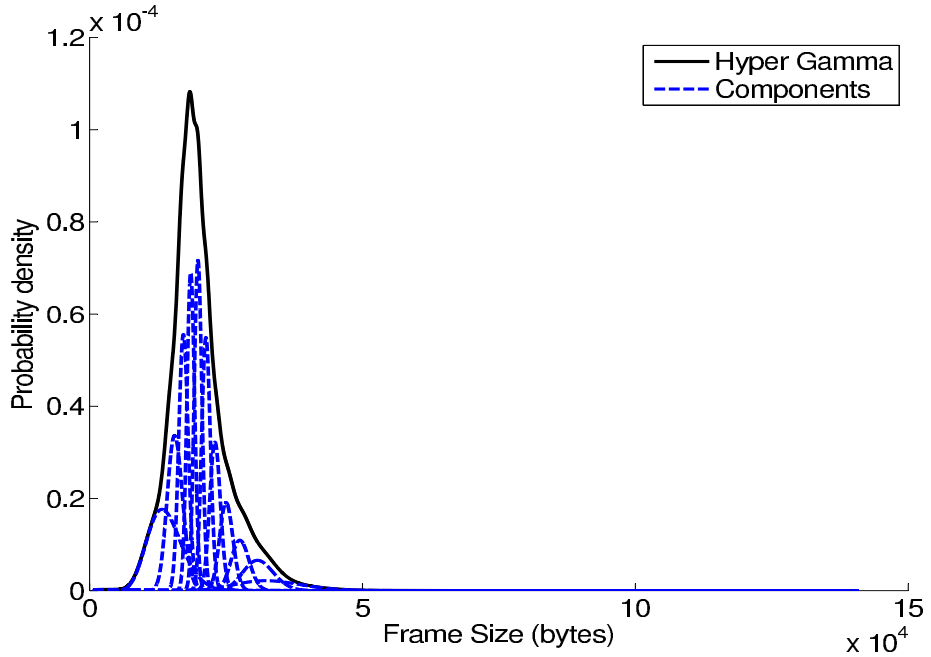

B Estimated Hyper-Gamma distribution and its components

Figure 3-4. Statistical characteristics(i.e. probability density function) of B-frame of the movie *Matrix*.

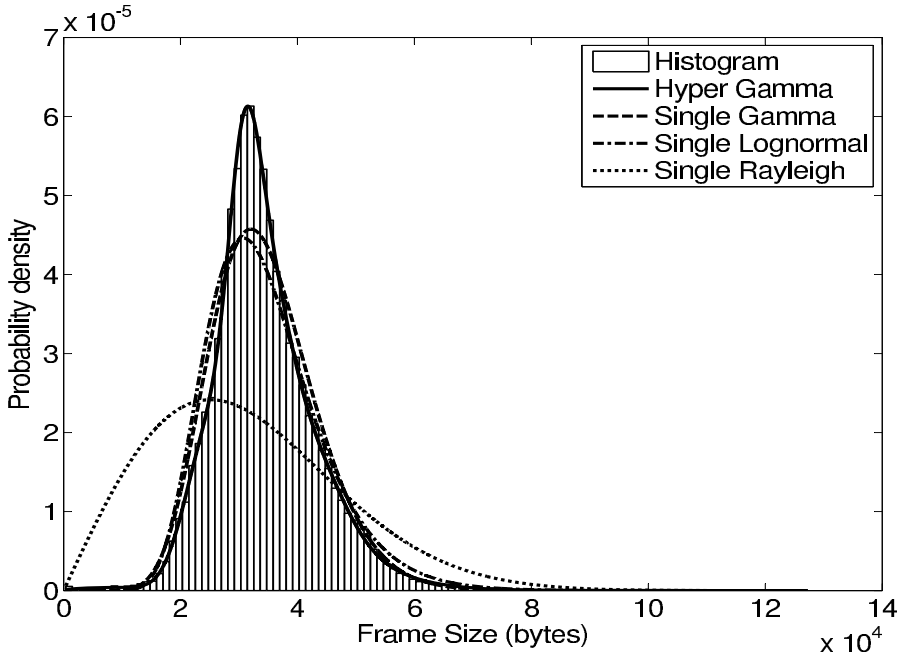

A Histogram, single density functions, and Hyper-Gamma density function

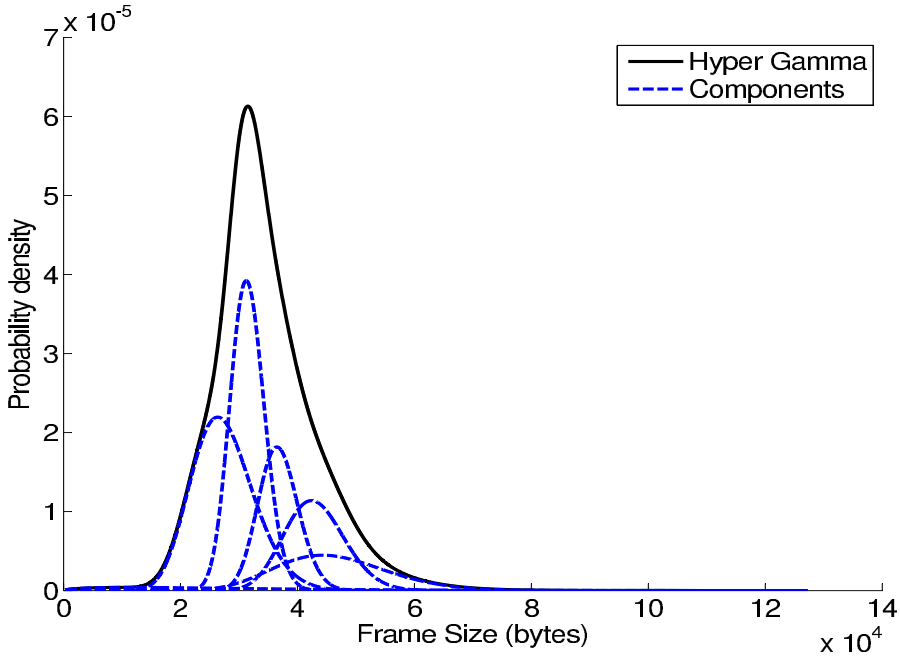

B Estimated Hyper-Gamma distribution and its components

Figure 3-5. Statistical characteristics(i.e. probability density function) of P-frame of the movie *Matrix*.

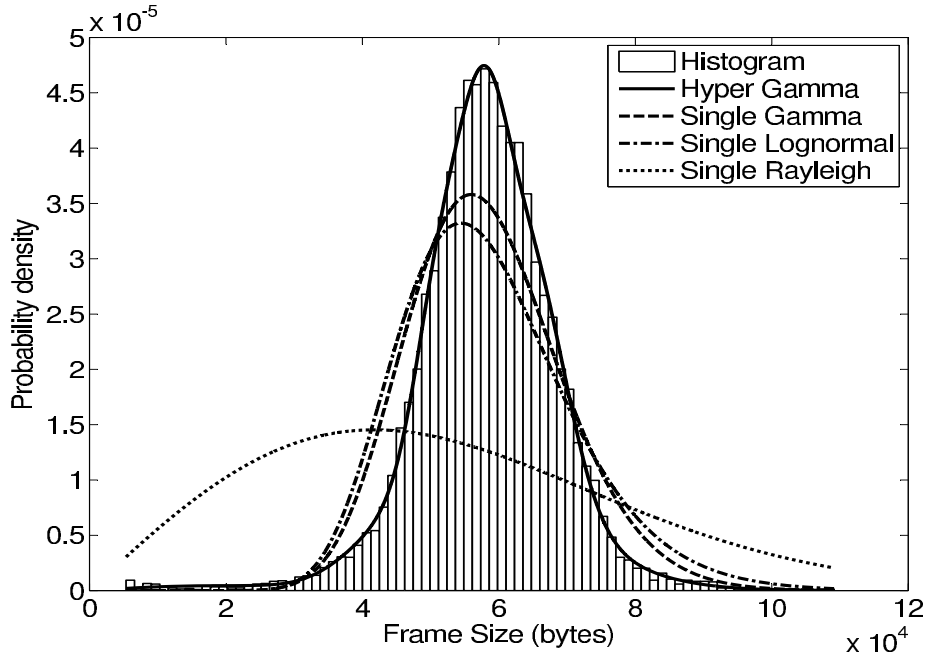

A Histogram, single density functions, and Hyper-Gamma density function

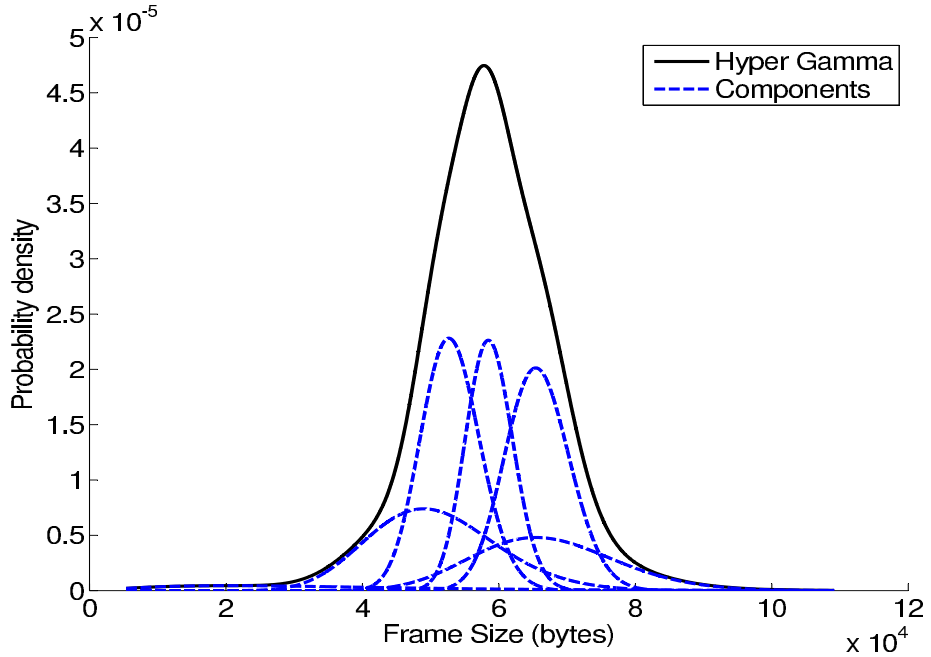

B Estimated Hyper-Gamma distribution and its components

Figure 3-6. Statistical characteristics(i.e. probability density function) of I-frame of the movie *Matrix*.

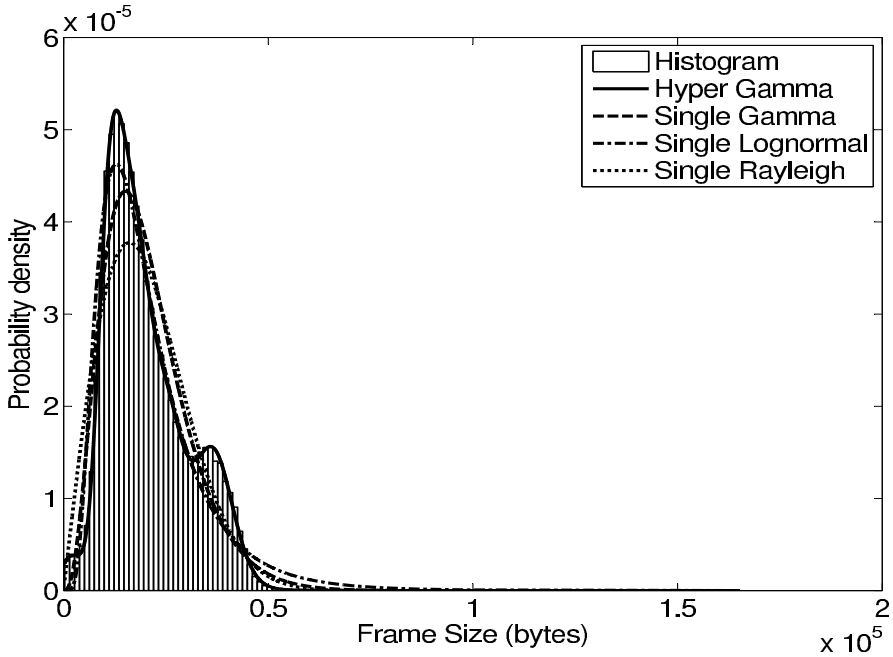

A Histogram, single density functions, and Hyper-Gamma density function

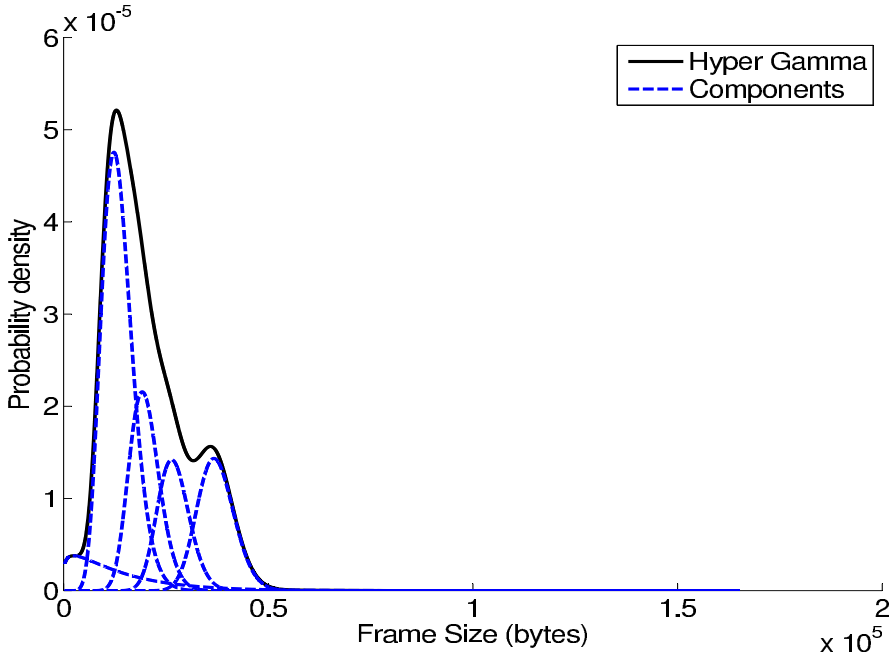

B Estimated Hyper-Gamma distribution and its components

Figure 3-7. Statistical characteristics(i.e. probability density function) of B-frame of the movie *Lord of the Rings II*.

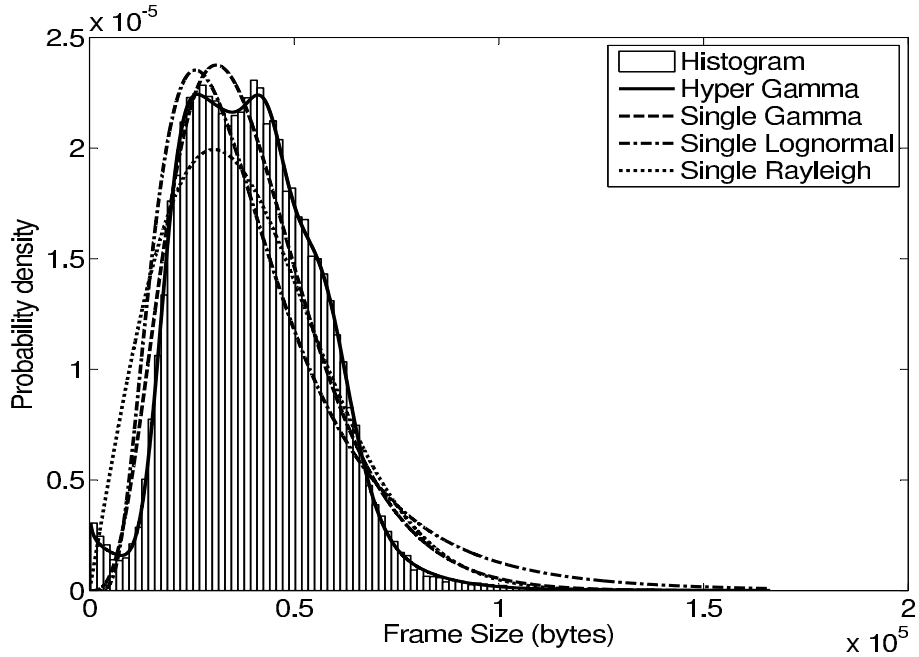

A Histogram, single density functions, and Hyper-Gamma density function

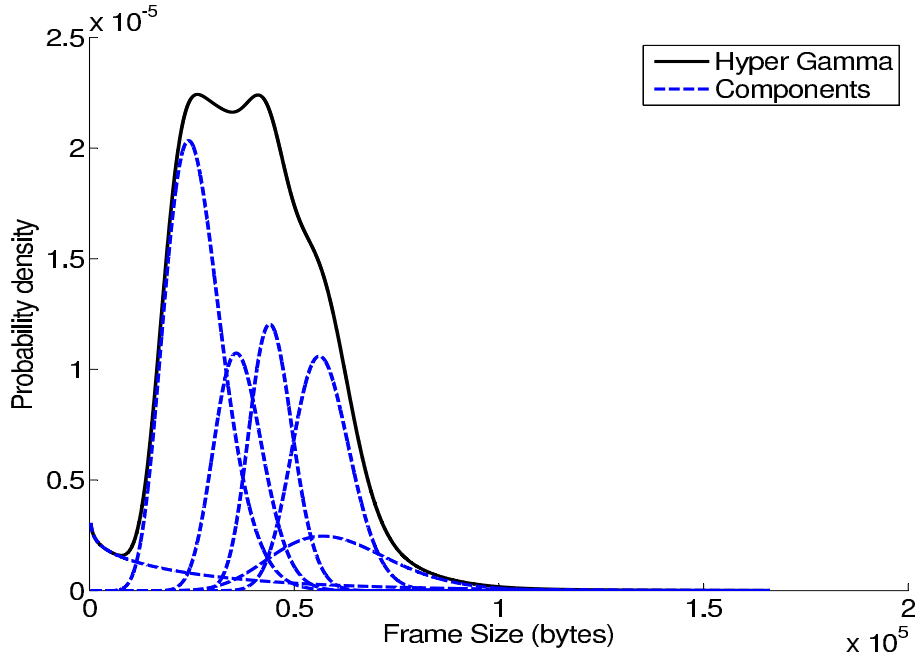

B Estimated Hyper-Gamma distribution and its components

Figure 3-8. Statistical characteristics(i.e. probability density function) of P-frame of the movie *Lord of the Rings II*.

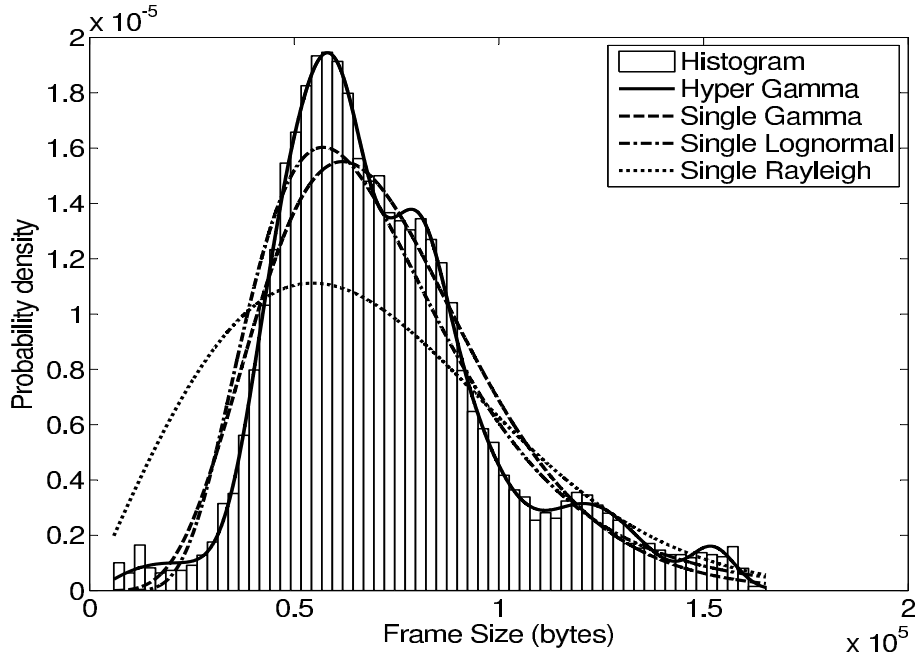

A Histogram, single density functions, and Hyper-Gamma density function

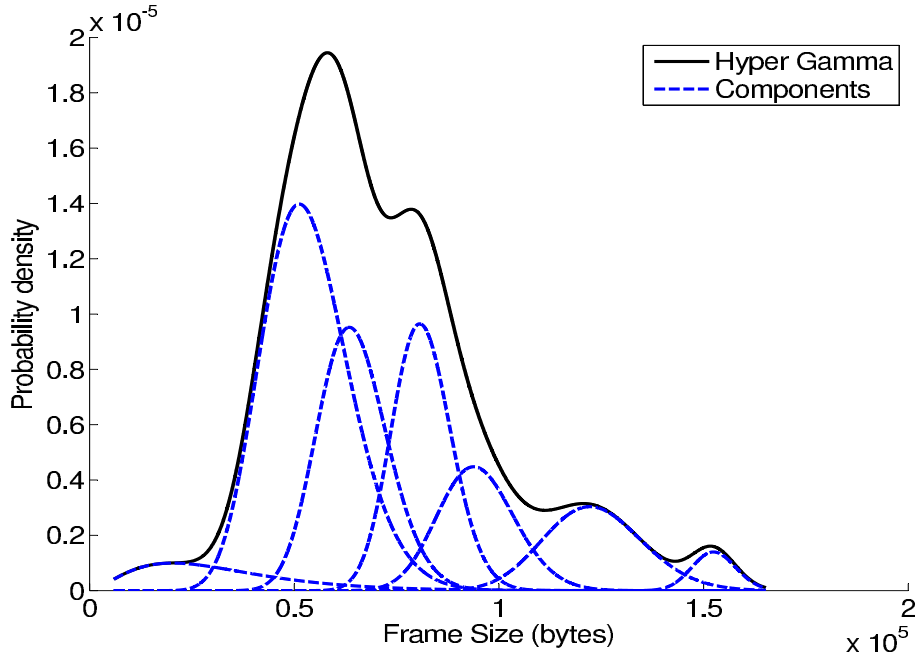

B Estimated Hyper-Gamma distribution and its components

Figure 3-9. Statistical characteristics(i.e. probability density function) of I-frame of the movie *Lord of the Rings II*.

CHAPTER 4
METHODS FOR AN ANALYSIS OF MULTIMEDIA TRAFFIC

4.1 Other Approach to Handling Multimedia Traffic: IEEE 802.11n

In this segment of the research we are interested in studying the performance of multimedia traffic over wireless mesh networks. In this regard, it is instructive to examine how multimedia traffic is handled by non-meshed wireless networks using the 802.11x suite of protocol. This information will prove usefulness as we examine the more complex wireless mesh structures. As mentioned in previous sections, the performance enhancement for network systems is the final goal of all researchers and engineers involved in the study of network systems. Thus, there have been evolved and introduced a number of technologies to satisfy the demand for higher performance local area network (LAN) systems and the one mainstream of the development of these technologies is the IEEE 802.11 standard series for a wireless LAN. If we have a careful look at the traffic types over communication networks, the multimedia traffic dominates over the whole communication network traffic due to its massiveness of size. In addition, when the multimedia information is transferred through a communication channel which has a physically limited capacity, there needs to make a consideration for guaranteeing a QoS of the transmission. In response to increasing this kind of demands for achieving enhanced performance WLANs, the Institute of Electrical and Electronics Engineers-Standards Association (IEEE-SA) has been making an amendment of the IEEE 802.11 standards.

Table 4-1. Wireless LAN throughput by IEEE Standard: Comparison of different 802.11 transfer rates.

IEEE WLAN Standard	Over-the-Air Estimates	Media Access Control Layer Service Access Point (MAC SAP) Estimates
802.11b	11 Mbps	5 Mbps
802.11g	54 Mbps	25 Mbps (when .11b is not present)
802.11a	54 Mbps	25 Mbps
802.11n	200+ Mbps	100 Mbps

802.11 (802.11 legacy) The IEEE 802.11 legacy is the original version of IEEE 802.11 standard which is released in 1997 and clarified in 1999. It support up to 2 Mbps data rate and forward error correction code. The 802.11 legacy standard defines three physical layers technologies; Direct-sequence spread spectrum (DSSS) operating in the 2.4 GHz ISM band, at data rates of 1Mbps and 2 Mbps, Frequency-hopping spread spectrum (FHSS) operating in the 2.4 GHz ISM band, at data rates of 1 Mbps and 2 Mbps, and Infrared operating at a wavelength between 850 and 950 nm, at 1 Mbps and 2 Mbps. Today, 802.11 legacy is out of date, but is renowned by IEEE 802.11b. [22]

802.11b The IEEE 802.11b standard is an extended version of the IEEE 802.11 legacy and uses the same media access technology specified in the IEEE 802.11 legacy. It supports the data rates from 5.5 Mbps to 11 Mbps. As the 802.11b standard directly extends the modulation technique specified in the 802.11 legacy standard, which is called complementary code keying, it can obtain a higher data rate in the same bandwidth compared to the 802.11 legacy standard and is the most widely used series of the 802.11 standard. [22, 23]

802.11a In case of the IEEE 802.11a standard, it employs an orthogonal frequency division multiplexing (OFDM) method as a modulation scheme for a transmission rather than a spread spectrum scheme as to increase the data rate. OFDM is known as a multicarrier modulation which uses a number of orthogonal subcarrier signals at closely spaced different frequencies and transmits some of bits on each channel. By using the OFDM technology, the 802.11a standard can obtain a high tolerance for severe channel conditions, where narrow band interference or frequency selective fading due to the multi-path effect (i.e. inter-channel interference) arises. The IEEE802.11a standard operates in the 5 GHz band and its possible data rates per channel are 6, 9, 12, 18, 24, 36, 48, and 54 Mbps.[22, 23]

802.11g The IEEE 802.11g standard which was ratified in June 2003 is an amended version of the IEEE 802.11b standard, which operates in the same base band 2.4 GHz as the 802.11b, so it is compatible with the 802.11b standard. The 802.11g standard allows the maximum data rate to up to 54 Mbps. The main difference between the standards 802.11g and 802.11b is the modulation technique. The standard 802.11g employs both OFDM and DSSM for its modulation methods, whereas the 802.11b uses only DSSM method. [22, 24]

802.11e In 2005, the IEEE-SA introduced another amended version of 802.11 standard which is called the 802.11e standard. The purpose of this amendment is to improve and guarantee the QoS for wireless LAN applications through modifications to the Media Access Control (MAC) layer. Thus, modules for a distributed coordination function (DCF) and point coordination function (PCF) are substituted for a hybrid coordination function (HCF) which is composed of enhanced distributed-channel access (EDCA) and HCF-controlled channel access (HCCA). By doing this, the 802.11e standard has better performance than the previous standards, where delay-sensitive applications such as voice over WLAN and streaming multimedia are used. [22]

802.11n The IEEE 802.11n standard is the latest amended version of the IEEE 802.11 standard. It has dramatically enhanced the capability of the data transmission rate (i.e. throughput) from 20 Mbps to around 200 Mbps in practice in accordance with the growing customer's demand for higher-performance wireless local area networks (WLANs). The emergence of the 802.11n standard is very desirable for the current market to satisfy the customer's needs for integrated services such as VOIP, real time video streaming, and entertainment multimedia, etc because these kinds of services are highly sensitive to the QoS. To fulfill the requests of the current market, the IEEE standard association employs the OFDM modulation

with the multiple-input multiple-output (MINO) antenna technology and 40 MHz bandwidth channels. [25, 26]

Table 4-1 shows the affordable throughput by the IEEE 802.11 standards. [27] When we consider the WLAN environments along with network traffic, the 802.11n standard is, recently, one of the remarkable enhanced technologies in obtaining higher throughput. The 802.11n standard makes it possible to extend a range of customer's demands; HDTV, online game services, DMB, a line of internet and multimedia-enabled smartphones, and etc, effectively. It could also guarantee the higher QoS than the previous series of the IEEE 802.11 standard. If we employ the 802.11n standard in their WLAN environment, we can take advantage of the benefits that it provides; the fast connection speed, the great, wide reaching range, though it is very expensive as compared with the other standards (i.e. 802.11 b/a/g) and always requires a MIMO adapter to be able to use its full potentials.

4.2 An Overview of Mesh Networks

The mesh network is a network, where each node can not only generate data for transmission from one node to another, but also relay data to other nodes through one or more channels and it has lately attracted considerable attention on the network and communication research society. [28–32] According to the topology of the mesh network, it can be categorized into two types of connection, full mesh topology or partial mesh topology. Figure 4-1 illustrate the two types of the mesh network topology. In case of the full mesh topology, all nodes are connected directly to each other, whereas the partial mesh topology allows the connection type that some nodes are connected to each other, but there are some of the nodes which are not connected each other. This topology can make the mesh network more reliable and provide much redundancy. When one node is not able to be functional, the rest of the nodes can still communicate with each other, directly or through one or more intermediate nodes. Therefore, the mesh network can maintain continuous connections and make a reconfiguration around

broken or blocked routes by hopping from node to node until information is delivered to the destination.

As data transmission in the mesh network arise in a multi-hop fashion from the source to the destination, we need to consider the hop-counts and the number of packets in the population of each node because the performance of mesh networks like throughput and delay depends on the hop-counts and its population of data within each node. In general, when the number of hop-count increases from the destination node, the per-node throughput may decrease, whereas end to end delay increases dramatically. This can cause the fairness problem in the mesh network; the nodes which have the small number of hop-counts from the destination node suffer from a lower throughput than the nodes closer to the destination node. [29, 33–35]

4.3 Analysis of the Dynamics of Mesh Networks: Jackson's Model

The section 4.2 provided an overview of mesh networks. Even though mesh networks have a good topological structure for the next generation network paradigm, it still has drawbacks to overcome; the fairness (i.e. throughput and delay performance). To improve the performance of mesh networks, there is a need to analyze the dynamic characteristics of mesh networks rigorously. One way of approach to the dynamics of mesh networks is a method which was introduced by Jackson. According to the

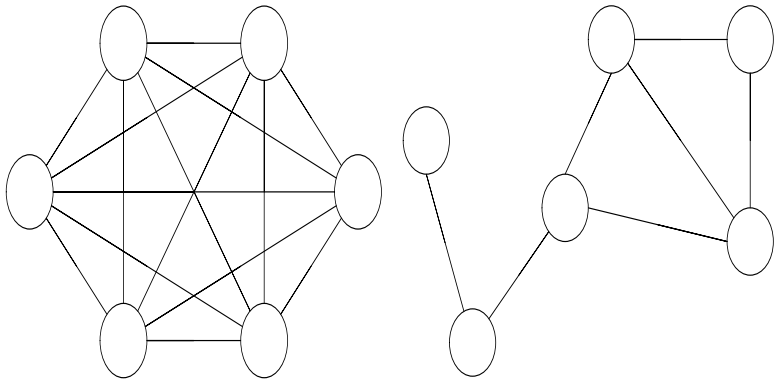

A Full mesh topology B Partial mesh topology

Figure 4-1. Mesh network topology.

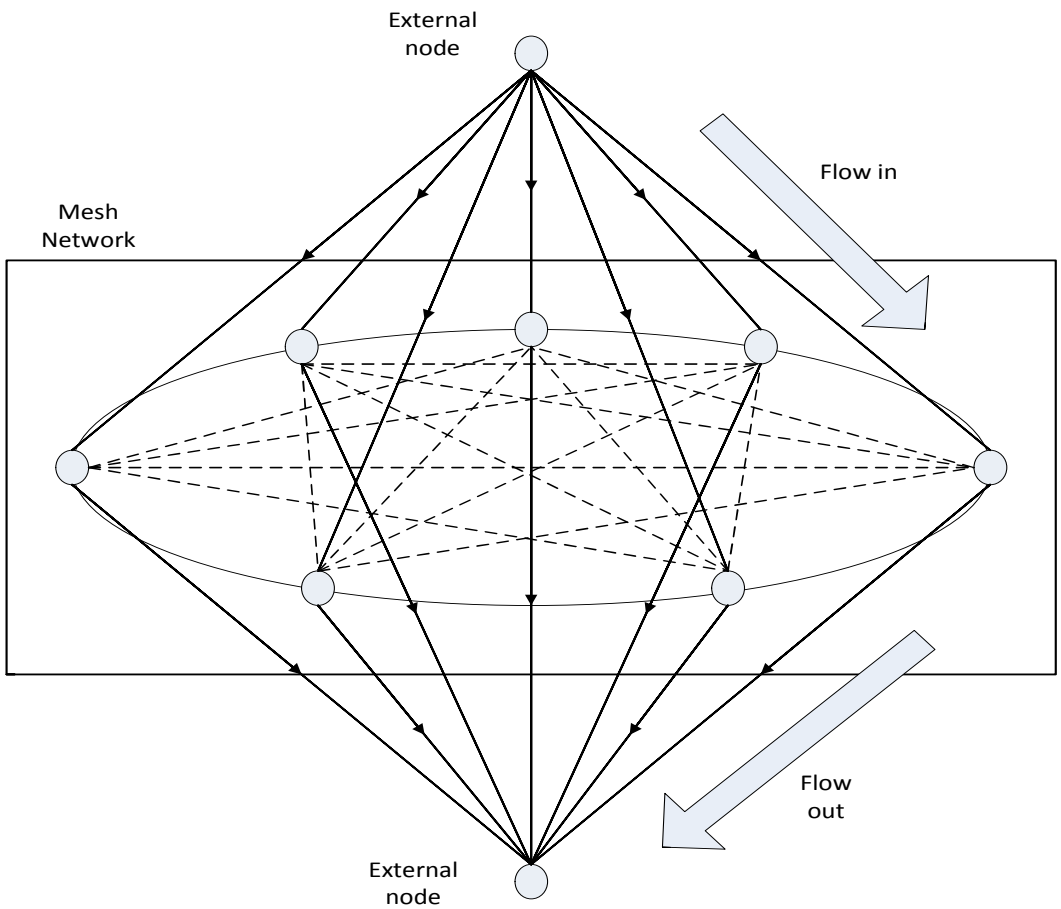

Figure 4-2. The topological structure of the Jackson network.

Jackson's theorem, a packet arrival process depends on the total number of packets in the network and service rate at any node may be a function of the number of packets in that node. [11, 36, 37] Let us consider the full mesh network depicted in Figure 4-2. There are N number of nodes in the system where the ith node has m_i exponential servers each with service rate parameter μ_{k_i}, where there are k_i packets at that node and define $S(\mathbf{k})$ as the total number of packets in the system, where the vector $\mathbf{k} = [k_1, k_2, \cdots, k_i, \cdots, k_N]$ represents the system state and k_i implies the number of packets in the ith node including the packet(s) in service. Moreover, we need to define a packet transition probability between nodes. r_{ij} denotes a transition probability of a packet from the ith node to the jth node, where $i, j = 1, 2, \cdots, N$. Then $r_{0,i}$ means a probability that the next externally generated arrival will enter the network at the ith node, $r_{i,N+1}$

implies a probability that a packet leaving node i departs from the network, and $r_{0,N+1}$ represents a probability that the next arrival will need no more service from the network and depart from the network instantly. Thus, an arrival rate from outside the system to the node i, γ_i is equal to $r_{0,i}\gamma(S(\mathbf{k}))$ and follows a Poisson process, where $\gamma(S(\mathbf{k}))$ denotes the total external arrival rate to the network when the network state is $S(\mathbf{k})$ at the moment. If we consider the time-dependent network state probabilities $P_{\mathsf{k}}(t)$, then a dynamic equation of the mesh network has the form as follows:

$$\begin{aligned}\frac{d}{dt}P_{\mathsf{k}}(t) = &-\left[\gamma(S(\mathbf{k})) + \sum_{i=1}^{N}\mu_{k_i}(1-r_{ii})\right]P_{\mathsf{k}}(t) + \sum_{i=1}^{N}\gamma(S(\mathbf{k})-1)r_{0,i}P_{\mathsf{k}(i^-)}(t)\\ &+\sum_{i=1}^{N}\mu_{k_i+1}r_{i,N+1}P_{\mathsf{k}(i^+)}(t) + \sum_{\substack{i=1\\ i\neq j}}^{N}\sum_{j=1}^{N}\mu_{k_j+1}r_{ji}P_{\mathsf{k}(i,j)}(t)\end{aligned} \tag{4–1}$$

where terms which have the negative vector arguments is equal to zero and notations denote that $\mathbf{k}(i^-) = [k_1, k_2, \cdots, k_i - 1, \cdots, k_N]$, $\mathbf{k}(i^+) = [k_1, k_2, \cdots, k_i + 1, \cdots, k_N]$, and $\mathbf{k}(i,j) = [k_1, k_2, \cdots, k_i - 1, \cdots, k_j + 1, \cdots, k_N]$ $(i \neq j)$.

To trace Equation (4–1), let us consider a simple birth-death process which is a Markov chain $X(t)$ with birth rate λ_k and death rate μ_k. Then $P_k(t)(= P[X(t) = k])$ can be explained as a probability that the population size is of k at arbitrary time t and the following probabilities are true based on the Markov property:

- P[exactly 1 birth in $(t, t+\Delta t)$ | k in population] = $\lambda_k\Delta t + o(\Delta t)$
- P[exactly 1 death in $(t, t+\Delta t)$ | k in population] = $\mu_k\Delta t + o(\Delta t)$
- P[exactly 0 birth in $(t, t+\Delta t)$ | k in population] = $1 - \lambda_k\Delta t + o(\Delta t)$
- P[exactly 0 death in $(t, t+\Delta t)$ | k in population] = $1 - \mu_k\Delta t + o(\Delta t)$

In other words, exactly one birth occurs in the interval $(t, t+\Delta t)$ means that there is no birth in $(0, t)$ and just one birth during the small time period Δt. Thus,

$$\begin{aligned} P\left[\tilde{t} \leq t+\Delta t | \tilde{t} > t\right] &= 1 - e^{-\lambda \Delta t} \\ &= 1 - [1 - \lambda \Delta t + \frac{(\lambda \Delta t)^2}{2!} - \cdots] \\ &= \lambda \Delta t + o(\Delta t) \end{aligned} \tag{4–2}$$

and the probability that no birth occurs in $(t, t+\Delta t)$ is

$$\begin{aligned} P\left[\tilde{t} > t+\Delta t | \tilde{t} > t\right] &= 1 - P\left[\tilde{t} \leq t+\Delta t | \tilde{t} > t\right] \\ &= 1 - \left(1 - e^{-\lambda \Delta t}\right) \\ &= e^{-\lambda \Delta t} \\ &= 1 - \lambda \Delta t + \frac{(\lambda \Delta t)^2}{2!} - \cdots \\ &= 1 - \lambda \Delta t + o(\Delta t) \end{aligned} \tag{4–3}$$

Finally, the probability that the two or more birth occur in the interval $(t, t+\Delta t)$ becomes

$$\begin{aligned} P\left[\textit{two or more births in } (t, t+\Delta t)\right] &= 1 - P\left[\textit{zero birth in } (t, t+\Delta t)\right] - P\left[\textit{one birth in } (t, t+\Delta t)\right] \\ &= 1 - (1 - \lambda \Delta t + o(\Delta t)) - (\lambda \Delta t + o(\Delta t)) \\ &= o(\Delta t) \end{aligned} \tag{4–4}$$

The same situation arise in the death process.

From Equation (4–1) to Equation (4–4), we can obtain a set of differential-difference equations which represent the dynamics of the birth-death network system.

$$\frac{d}{dt} P_k(t) = -\left(\lambda_k + \mu_k\right) P_k(t) + \lambda_{k-1} P_{k-1}(t) + \mu_{k+1} P_{k+1}(t) \quad \text{for } k \geq 1 \tag{4–5a}$$

$$\frac{d}{dt} P_0(t) = -\lambda_0 P_0(t) + \mu_1 P_1(t) \quad \text{for } k = 0 \tag{4–5b}$$

Now, going back to Equation (4–1), let us consider a change of probability during a small amount of interval Δt. This quantity is given as follows:

$$P_{\mathsf{k}}(t+\Delta t) = \left[1 - \gamma(S(\mathbf{k}))\Delta t - \sum_{i=1}^{N} \mu_{k_i}(1-r_{ii})\Delta t\right] P_{\mathsf{k}}(t) + \sum_{i=1}^{N} \gamma(S(\mathbf{k})-1) r_{0,i} \Delta t P_{\mathsf{k}(i^-)}(t) + \sum_{i=1}^{N} \mu_{k_i+1} r_{i,N+1} \Delta t P_{\mathsf{k}(i^+)}(t) + \sum_{\substack{i=1 \\ i\neq j}}^{N} \sum_{j=1}^{N} \mu_{k_j+1} r_{ji} \Delta t P_{\mathsf{k}(i,j)}(t) \tag{4–6}$$

If we subtract $P_{\mathsf{k}}(t)$, divide by Δt both sides and take the limit as $\Delta t \to 0$, then we, finally, obtain Equation (4–1).

Jackson already stated that the solution of Equation (4–1), a joint probability of state description is a product of its marginal distribution of finding k_i packets in the ith node given by $p_i(k_i)$.

$$p(k_1, k_2, \cdots, k_N) = p(k_1)p(k_2)\cdots p(k_N) \tag{4–7}$$

where $p_i(k_i)$ is a probability of finding k_i packets in the classical $M/M/m$ queueing system. [11]

4.4 Results and Discussion

In general, when we are trying to obtain dynamic behavior for network systems and analyze it, if we have the exponential assumptions for an arrival process and service time distribution, then we can analyze the network system by using the Jackson's theorem and he said that a joint probability of state description is a product of its marginal distribution of finding k_i packets in the ith node. Unfortunately, the lack of the exponential assumption in a service time distribution for multimedia traffic in a real world could not make it possible to build an analytical and tractable model for mesh networks. Thus we need to consider another method to obtain performance factors like throughput and delay of network systems based on multimedia traffic.

CHAPTER 5
AN APPROACH TO THE PERFORMANCE ANALYSIS FOR NETWORK SYSTEMS BASED ON MULTIMEDIA TRAFFIC

5.1 An Overview of the Hyper-Gamma Service Time Distribution

Up to this point, we have studied the statistical multimedia traffic model from real movie data, especially encoded in MPEG-2. Based on an extensive investigation of movie frames, it turns out that the statistical model for each DVD movie frame contributing to multimedia traffic follows the Hyper-Gamma distribution and it, more specifically, implies that a probability density function of the frame size of commercial DVD movies is the Hyper-Gamma distribution which is specified in Equation (3–1). It is also directly related to a service time distribution in network systems. In other words, we agree that we may intuitively know the fact that the service time required to a node to handle movie frames in network systems is proportional to the size of movie frames and also follows the Hyper-Gamma distribution. Furthermore, this type of network system is relevant to a non-Markovian stochastic process for a network model because of relaxation for an exponential assumption in a service time distribution. Thus, in order to obtain performance measures, like throughput and delay of network systems based on multimedia traffic, we have to approach these network systems with one of general types of a service time distribution, that is, the Hyper-Gamma service time distribution model (i.e. M/HG/1 queueing network). After completing the analysis of a single node M/HG/1 system, we will apply the results of the M/HG/1 system to a series (or tandem) network to obtain network performance factors, namely, throughput and delay.

5.2 A Background for Network Systems with the Hyper-Gamma Service Time Distribution

The results in Chapter 3 describe the fact that the service time distribution for multimedia traffic in network systems follows the Hyper-Gamma distribution which is expressed in Equation (3–1) and has no longer Markovian properties. This makes it a bit cumbersome to analyze network systems based on multimedia traffic. Moreover, since

we do not have information about the arrival process in real network systems yet, we assume that the arrival process to a network node follows a Poisson process. Thus we have an M/HG/1 system which is defined as a single server system with Poisson arrivals with an average rate of λ frames per second, a mean interarrival time of $1/\lambda$ second and a Hyper-Gamma service time distribution. Furthermore, a system utilization factor should be less than one for a stability of network systems.

$$\rho = \lambda E_{hygam}[X] \tag{5–1}$$

We can now rewrite the density function of the Hyper-Gamma distribution which represents the service time distribution for multimedia traffic in network systems.

$$f_{hygam}(x) = \sum_{i=1}^{N} \alpha_i \frac{\beta_i^{k_i}}{\Gamma(k_i)} x^{k_i-1} e^{-\beta_i x} \qquad x > 0 \tag{5–2}$$

The only difference between Equation (3–1) and Equation (5–2) is a set of scale parameters, namely, $\beta_i = 1/\theta_i$ for $i = 1, 2, \cdots, N$. We also rewrite the Laplace transform of the Hyper-Gamma distribution as follows:

$$\begin{aligned} F^L_{hygam}(s) &= \int_0^\infty f_{hygam}(x) e^{-sx} dx \\ &= \int_0^\infty \sum_{i=1}^{N} \alpha_i \frac{\beta_i^{k_i}}{\Gamma(k_i)} x^{k_i-1} e^{-\beta_i x} e^{-sx} dx \\ &= \sum_{i=1}^{N} \alpha_i \frac{\beta_i^{k_i}}{\Gamma(k_i)} \int_0^\infty x^{k_i-1} e^{-(\beta_i+s)x} dx \\ &= \sum_{i=1}^{N} \alpha_i \frac{\beta_i^{k_i}}{\Gamma(k_i)} \frac{1}{(\beta_i+s)^{k_i}} \int_o^\infty y^{k_i-1} e^{-y} dy \\ &= \sum_{i=1}^{N} \alpha_i \beta_i^{k_i} (\beta_i + s)^{-k_i} \end{aligned} \tag{5–3}$$

When we are trying to analyze these kinds of systems, we must consider a vector state description $[N(t), X_0(t)]$ which describes the number of frames in the system at

time *t*, denoted by $N(t)$, and the service time already received by the frame in service at time *t*, denoted by $X_0(t)$. But if we look at the system at the instant of a frame departure from the service (or the system), then the state description can be reduced to $N(t)$ since the expended service time, $X_0(t)$ at this instant is equal to zero for a frame in service because it just entered the service. This is the fundamental idea behind the method of the imbedded Markov chain in which the departure instant corresponds to an imbedded point. Indeed, we already know for a fact that Equation (5–4) is always true for a Poisson process due to the PASTA (Poisson Arrivals See Time Averages) property [38].

$P_k(t) = P[N(t) = k]$: the number of frames in system at time *t*

$R_k(t) = P$ [*arrival at time* t *finds* k *frames in system*]

$$P_k(t) = R_k(t) \tag{5–4}$$

Moreover, on average, the limit of the following distributions are also identical in the M/HG/1 system.

$p_k = \lim_{t\to\infty} P$ [*the number of frames in system at time* t]

$r_k = \lim_{t\to\infty} P$ [*an arrival finds* k *frames in system at time* t]

$d_k = \lim_{t\to\infty} P$ [*a departure leaves* k *frames in system at time* t]

$$r_k = d_k \tag{5–5}$$

$$\therefore r_k = d_k = p_k \tag{5–6}$$

Consequently, the arrival frames to the system, departure frames from the system and outside frames looking into the system all see the same distribution of the number of frames in the M/HG/1 system. [11, 39]

Let us now consider three random variables ξ_n, x_n, and ϕ_n. First, ξ_n is defined as the number of frames left behind by a departure of the nth frame from service. Thus $P[\xi_n = k]$ implies a probability of *k* numbers of frames in the system just after

a departure of the nth frame and its limit form ($n \to \infty$) corresponds to d_k. According to Equation (5–6), the probability p_k (=$P[\widetilde{\xi} = k]$) which implies the average number of frames in system is equal to d_k. Next, x_n is the service time for the nth frame, which is distributed according to $F_{hygam}(x)$ as appeared in Equation (3–3) and is independent of n. And the last one, ϕ_n is the number of frames arriving during the service time x_n of the nth frame and depends only on the length of x_n, not on n. The limiting distributions of the three random variables (ξ_n, x_n, and ϕ_n) are expressed as $\widetilde{\xi}$, $\widetilde{x}$, and $\widetilde{\phi}$. Furthermore we define a random variable a_k as a probability that exactly k frames arrive during the service time of a frame.

$$\begin{aligned} a_k &= P[\widetilde{\phi} = k] \\ &= \int_0^\infty \frac{(\lambda x)^k}{k!} e^{-\lambda x} f_{hygam}(x) dx \end{aligned} \tag{5–7}$$

Additionally, we have to define the one-step transition probabilities which is observed only at the departure instant.

$$p_{ij} = P[\xi_{n+1} = j | \xi_n = i] \tag{5–8}$$

Obviously, p_{ij} equals zero for all $j < i-1$ and p_{ij} is the probabilities that exactly $(j-i+1)$ frames arrived during the service time of the $(k+1)$th frame for $j \geq i-1$, given that the nth frame left behind exactly i frames. Thus a transition probability matrix is given as follows:

$$P = \begin{bmatrix} a_0 & a_1 & a_2 & a_3 & \cdots \\ a_0 & a_1 & a_2 & a_3 & \cdots \\ 0 & a_0 & a_1 & a_2 & \cdots \\ 0 & 0 & a_0 & a_1 & \cdots \\ 0 & 0 & 0 & a_0 & \cdots \\ \vdots & \vdots & \vdots & \vdots & \ddots \end{bmatrix} \tag{5–9}$$

Let us now try to obtain the average queue length at frame departure instants which can be represented as $E[\widetilde{\xi}]$. Before doing this, we have to find the relationship between two random variables, ξ_{n+1} and ξ_n. In order to find an equation relating ξ_{n+1} and ξ_n, we must consider two cases at the instant of the nth frame departure, which means that the departure of the nth frame leaves behind a non-empty system and an empty system. In the non-empty system case ($\xi_n > 0$), the $(n+1)$th frame is already in the system when the nth frame departs. In the other case ($\xi_n = 0$), since the departing frame leaves behind an empty system, ξ_{n+1} is equal to the number of arrivals in its service time. Thus, we have Equation (5–10).

$$\xi_{n+1} = \xi_n - D_{\xi_n} + \phi_{n+1} \tag{5–10}$$

D_k is defined as follows:

$$D_k = \begin{cases} 1 & \textit{for} \quad k > 0 \\ 0 & \textit{for} \quad k \leq 0 \end{cases} \tag{5–11}$$

We now make an expectation of both sides of Equation (5–10) and taking the limit as n goes to infinity, then we have

$$E[D_{\widetilde{\xi}}] = E[\widetilde{\phi}] \tag{5–12}$$

Since $\widetilde{\phi}$ means the number of arrivals during a frame's service time which is independent of n, $E[\widetilde{\phi}]$ implies the average number of arrivals in a service time. Moreover, the left-hand side of Equation (5–12) is given as follows and represents a probability that the system is busy.

$$\begin{aligned} E[D_{\widetilde{\xi}}] &= \sum_{k=0}^{\infty} D_k P[\widetilde{\xi} = k] \\ &= 0 \cdot P[\widetilde{\xi} = 0] + 1 \cdot P[\widetilde{\xi} > 0] \\ &= P[\widetilde{\xi} > 0] \end{aligned} \tag{5–13}$$

The last term of Equation (5–13) also implies the probability of a busy system and can be interpreted as a system utilization factor ρ. Thus, the average number of arrivals per

service interval is identical to ρ and also can be represented in terms of the average service time.

$$E[D_{\widetilde{\xi}}] = E[\widetilde{\phi}] = \rho = \lambda E[\widetilde{x}] \tag{5–14}$$

Let us now proceed with a method for obtaining all the moments of a random variable $\widetilde{\phi}$ in equilibrium. In order to do so, we define first the moment generating function $\Phi(z)$ which is a z-transform for the random variable $\widetilde{\phi}$.

$$\Phi(z) \triangleq E[z^{\widetilde{\phi}}] \triangleq \sum_{k=0}^{\infty} P[\widetilde{\phi} = k] z^k \tag{5–15}$$

Thus,

$$\begin{aligned}
\Phi(z) &= \sum_{k=0}^{\infty} P[\widetilde{\phi} = k] z^k \\
&= \sum_{k=0}^{\infty} \int_0^{\infty} \frac{(\lambda x)^k}{k!} e^{-\lambda x} f_{hygam}(x) dx \cdot z^k \\
&= \int_0^{\infty} e^{-\lambda x} \left(\sum_{k=0}^{\infty} \frac{(\lambda x z)^k}{k!} \right) f_{hygam}(x) dx \\
&= \int_0^{\infty} e^{-\lambda x} e^{\lambda x z} f_{hygam}(x) dx \\
&= \int_0^{\infty} e^{-(\lambda - \lambda z)x} f_{hygam}(x) dx
\end{aligned} \tag{5–16}$$

$F^L_{hygam}(s)$ denotes the Laplace transform of the Hyper-Gamma distribution which is a service time distribution as appeared in Equation (5–3). Thus we have

$$\Phi(z) = F^L_{hygam}(\lambda - \lambda z) \tag{5–17}$$

Equation (5–14) give us an insight that the random variable $\widetilde{\phi}$ implies the number of arrivals during the service time interval $\widetilde{x}$ where the arrival process is Poisson at an average arrival rate of λ frames per second. The nth moment of the service time distribution is given in Equation (3–5) and we already know the relationship between the

z-transform and the Laplace transform, namely, $s = 0$ corresponds to $z = 1$. Thus we have

$$F_{hygam}^{L}{}^{(k)}(s) = (-1)^k \frac{d^k}{ds^k} F_{hygam}^{L}(s)\Big|_{s=0} = (-1)^k E[\widetilde{x}^k] \tag{5–18}$$

$$\Phi^{(1)}(1) = \frac{d}{dz}\Phi(z)\Big|_{z=1} = E[\widetilde{\phi}] \tag{5–19}$$

$$\Phi^{(2)}(1) = \frac{d^2}{dz^2}\Phi(z)\Big|_{z=1} = E[\widetilde{\phi}^2] - E[\widetilde{\phi}] \tag{5–20}$$

and

$$F_{hygam}^{L}(0) = \Phi(1) = 1 \tag{5–21}$$

If we investigate the second moment of the random variable $\widetilde{\phi}$, from Equation (5–18) and Equation (5–20), we can obtain the following relationship.

$$\begin{aligned}
\Phi^{(2)}(1) &= \frac{d^2}{dz^2}\Phi(z) \\
&= \frac{d^2}{dz^2} F_{hygam}^{L}(\lambda - \lambda z) \\
&= \frac{d}{dz}\left[-\lambda \frac{d}{dy} F_{hygam}^{L}(y)\right] \\
&= -\lambda \frac{d^2}{dy^2} F_{hygam}^{L}(y) \frac{dy}{dz} \\
&= \lambda^2 \frac{d^2}{dy^2} F_{hygam}^{L}(y)\Big|_{y=0} \\
&= \lambda^2 F_{hygam}^{L}{}^{(2)}(0) \\
&= \lambda^2 E[\widetilde{x}^2] \\
&= E[\widetilde{\phi}^2] - E[\widetilde{\phi}]
\end{aligned} \tag{5–22}$$

where we let y be $\lambda - \lambda z$.

We now attempt to find the average queue size $E[\widetilde{\xi}]$ at frame departure instants by squaring Equation (5–10).

$$\xi_{n+1}^2 = \xi_n^2 + D_{\xi_n}{}^2 + \phi_{n+1}^2 - 2\xi_n D_{\xi_n} + 2\xi_n \phi_{n+1} - 2D_{\xi_n}\phi_{n+1} \tag{5–23}$$

where $(D_{\xi_n})^2$ equals D_{ξ_n} and $\xi_n D_{\xi_n}$ is identical to ξ_n from Equation (5–11). Also the number of arrivals during the (n+1)th service interval is independent of the number of frames left behind by the nth frame.

Now if we make an expectation on both sides and take a limit, then we have

$$0 = E[D_{\widetilde{\xi}}] + E[\widetilde{\phi}^2] - 2E[\widetilde{\xi}] + 2E[\widetilde{\xi}]E[\widetilde{\phi}] - 2E[D_{\widetilde{\xi}}]E[\widetilde{\phi}] \tag{5–24}$$

From Equations (5–14), (5–17) and (5–22), we have

$$\begin{aligned} E[\widetilde{\xi}] &= \rho + \frac{E[\widetilde{\phi}^2] - E[\widetilde{\phi}]}{2(1-\rho)} \\ &= \lambda E[\widetilde{x}] + \frac{\lambda^2 E[\widetilde{x}^2]}{2(1-\lambda E[\widetilde{x}])} \end{aligned} \tag{5–25}$$

Consequently, from Equations (3–7) and (3–8), we have the average number of frames in the system for multimedia traffic which is specified by Poisson arrival process at an average rate of λ frames per second and have the Hyper-Gamma service time distribution with a single server is given as follows:

$$E[\widetilde{\xi}] = \lambda \sum_{i=1}^{N} \alpha_i k_i \theta_i + \frac{\lambda^2 \sum_{i=1}^{N} \alpha_i k_i (k_i+1) {\theta_i}^2}{2(1 - \sum_{i=1}^{N} \alpha_i k_i \theta_i)} \tag{5–26}$$

Let us now examine Little's law.

$$\overline{N} = \lambda T \tag{5–27}$$

where $\overline{N}$ is the average number of frames in the system (including a frame in service) and and T is the average time spent in the system (queueing time + service time). Thus, from Equation (5–25), we have

$$\overline{N} = E[\widetilde{\xi}] = \lambda E[\widetilde{x}] + \frac{\lambda^2 E[\widetilde{x}^2]}{2(1-\lambda E[\widetilde{x}])} = \lambda T \tag{5–28}$$

$$T = E[\widetilde{x}] + \frac{\lambda E[\widetilde{x}^2]}{2(1-\lambda E[\widetilde{x}])} \tag{5–29}$$

Clearly, we can make sure that the average time spent in the system is identical to the sum of the average time spent in the service and the average time spent in the queue from Equation (5–29). If we apply Equation (5–29) to our system which follows a Poisson arrival process at a rate of λ frames per second and a Hyper-Gamma service time distribution, then we have

$$T = \sum_{i=1}^{N} \alpha_i k_i \theta_i + \frac{\lambda \sum_{i=1}^{N} \alpha_i k_i (k_i + 1) {\theta_i}^2}{2(1 - \sum_{i=1}^{N} \alpha_i k_i \theta_i)} \tag{5–30}$$

If we want to obtain the the average number of frames in the queue, $\overline{N}_q$, (not including the frame in service), then we have to start with the definition of $\overline{N}$.

$$\overline{N} = E[\widetilde{\xi}] = \sum_{k=0}^{\infty} k P[\widetilde{\xi} = k] \tag{5–31}$$

Thus,

$$\begin{aligned} \overline{N}_q &= \sum_{k=1}^{\infty} (k-1) P[\widetilde{\xi} = k] \\ &= \sum_{k=1}^{\infty} \{k P[\widetilde{\xi} = k] - P[\widetilde{\xi} = k]\} \\ &= \sum_{k=0}^{\infty} k P[\widetilde{\xi} = k] - \sum_{k=1}^{\infty} P[\widetilde{\xi} = k] \\ &= \overline{N} - \rho \end{aligned} \tag{5–32}$$

Finally, let us go after the limiting distribution for ξ_n which is represented by $p_k (= P[\widetilde{\xi} = k])$ in the system. Actually, we know that the probability d_k of finding k frames in the system just after the departure of a frame, is equal to p_k from Equation (5–6). The first step that we have to do is to define the z-transform for the random variable ξ_n and its limiting random variable $\widetilde{\xi}$.

$$Q_n(z) \triangleq E[z^{\xi_n}] \triangleq \sum_{k=0}^{\infty} P[\xi_n = k] z^k \tag{5–33}$$

$$Q(z) \triangleq \lim_{n\to\infty} Q_z(z) = \sum_{k=0}^{\infty} P[\widetilde{\xi} = k] z^k = E[z^{\widetilde{\xi}}] \tag{5–34}$$

Moreover, the M/HG/1 queueing system is specified by Equation (5–10). Thus, we put both sides of Equation (5–10) to an exponent for z and take an expectation.

$$z^{\xi_{n+1}} = z^{\xi_n - \Delta_{\xi_n} + \phi_{n+1}} \tag{5–35}$$

$$E[z^{\xi_{n+1}}] = Q_{n+1}(z) = E[z^{\xi_n - \Delta_{\xi_n} + \phi_{n+1}}] \tag{5–36}$$

Since two random variables ξ_n and ϕ_{n+1} are independent each other, functions of independent random variables are also independent, and we have defined $\Phi(z)$ in Equation (5–15) such that $\Phi(z) = E[z^{\widetilde{\phi}}] = E[z^{\phi_{n+1}}]$, we can have the following form.

$$Q_{n+1}(z) = \Phi(z) E[z^{\xi_n - \Delta_{\xi_n}}] \tag{5–37}$$

Now, we take a look at the term $E[z^{\xi_n - \Delta_{\xi_n}}]$.

$$\begin{aligned} E[z^{\xi_n - \Delta_{\xi_n}}] &= \sum_{k=0}^{\infty} P[\xi_n = k] z^{k - \Delta_k} \\ &= P[\xi_n = 0] + \sum_{k=1}^{\infty} P[\xi_n = k] z^{k-1} \\ &= P[\xi_n = 0] + \frac{\sum_{k=0}^{\infty} P[\xi_n = k] z^k - P[\xi_n = 0]}{z} \\ &= P[\xi_n = 0] + \frac{Q_n(z) - P[\xi_n = 0]}{z} \end{aligned} \tag{5–38}$$

Thus, if we put Equation (5–38) into Equation (5–37), take the limit on both sides and solve it for $Q(z)$, then we finally have Equation (5–39) for $Q(z)$, namely, the z-transform for the number of frames in the infinite capacity system

$$\begin{aligned} Q(z) &= \Phi(z) P[\widetilde{\xi} = 0] + \frac{Q(z) - P[\widetilde{\xi} = 0]}{z} \\ &= \Phi(z) \frac{(1-\rho)(1-z)}{\Phi(z) - z} \\ &= F^L_{hygam}(\lambda - \lambda z) \frac{(1-\rho)(1-z)}{F^L_{hygam}(\lambda - \lambda z) - z} \end{aligned} \tag{5–39}$$

where the probability $p_0(= P[\widetilde{\xi} = 0])$ implies the empty system and is equal to $1 - \rho$.

5.3 Throughput and Delay for Network Systems Based on Multimedia Traffic

So far, what we have obtained is to analyze the performance of network systems which is specified by multimedia traffic. Let us now consider the mesh network in which we assume that a routing path has already been established. Although a node in mesh networks plays both roles of a client and a relay center, we assume that all nodes in mesh networks work only as an intermediate node, namely, a relay center in which they cannot generate their own frames for multimedia traffic, since there is usually just one source for a user to request or access to a multimedia source. We also assume that the arrival process for multimedia traffic follows a Poisson process at a rate of λ frames per second since we do not have information about the arrival process in real network systems yet and all nodes in mesh networks are identical. Furthermore, we also assume that the type of data flow is one way traffic which means that the traffic stream is one of up-streaming or down-streaming, though there exists a bidirectional stream (i.e. video conference). We also consider the situation which is depicted in Figure 4-2. For example, the upper external node is considered as a kind of video source node and the bottom external node is to be a user who wants to request a streaming service for a movie. Additionally, the order in which frames are taken from the queue, allowed into service, and departure from the system follows the First In First Out (FIFO) service discipline one by one. Consequently, based on the above assumptions, we can configure a tandem multimedia traffic network as depicted in Figure 5-1, where the source node and the destination node correspond to the upper external node and a user, respectively. Let us now attempt to find throughput and delay which are contributing to the performance of network systems based on multimedia traffic. As described in section 1.2, throughput of a network system is defined as the average rate with which frames are successfully transferred through the channel and delay can be considered as a sum of average waiting times in queues and service times

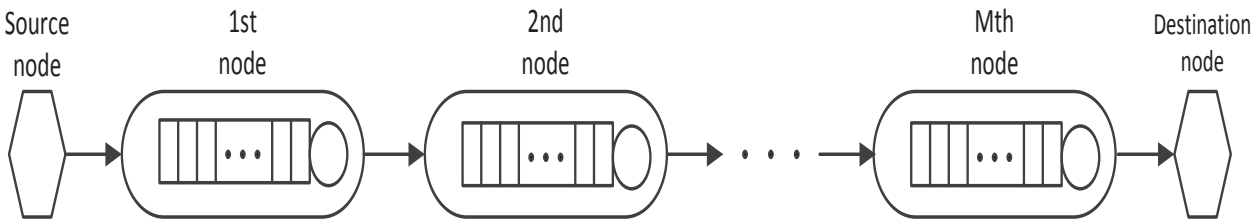

Figure 5-1. Infinite capacity network systems based on multimedia traffic after building a routing path.

in network nodes. Moreover, in case of the M/HG/1 system, we know for a fact that the average arrival rate to a node is equal to the average departure rate from the node from Equation (5–6) and each node has an infinite capacity, so there is no possibility to drop arriving frames to any nodes. Therefore, the average arrival rate to a node is identical to the average departure rate from that node and this departure rate becomes an average arrival rate to the next node and so on. Consequently, throughput of the M/HG/1 system is identical to the average arrival rate to the first node, λ. The next one we have to consider is delay. The above definition is considered only at a single node. But, in a viewpoint of a user or a destination node, delay is considered as a total time spent from the time when the source node starts to send a frame to the time until the destination node receives the frame. Since the arrival process follows a Poisson process at a rate of λ, the interarrival time of each frames is equal to $1/\lambda$. Therefore, in the case of the network as in Figure 5-1 which has M intermediate nodes, the total time spent (i.e. delay, T_{total}) from the source node to the destination node is

$$T_{total} = \frac{(M+1)}{\lambda} + M\left[\sum_{i=1}^{N}\alpha_i k_i \theta_i + \frac{\lambda\sum_{i=1}^{N}\alpha_i k_i (k_i+1){\theta_i}^2}{2(1-\sum_{i=1}^{N}\alpha_i k_i \theta_i)}\right] \tag{5–40}$$

In Equation (5–40), the term in the square brackets comes from Equation (5–30) which represents a total time spent (queue and service) at a node in the M/HG/1 system.

Let us now examine network systems (i.e. M/HG/1/K) based on multimedia traffic, which has nodes with a finite capacity of size K (queue + service). All other

assumptions remains the same as the case of network systems with an infinite capacity of size. This kind of system is more practical for real network systems because the infinite capacity for a node of networks cannot be implementable. The main feature of this system is that all nodes in the system can hold, at most, a total of K frames which includes a frame in service and any further arriving frames will be blocked and may be considered as a lost frame. Thus, an actual arrival rate λ_a is only a fraction of the average arrival rate λ and is equal to the actual departure rate λ_d with the same situation in Equation (5–6)

$$\lambda_a = \lambda(1 - P_B) = \lambda_d \tag{5–41}$$

where P_B is a blocking probability due to the limitation of a node capacity K. Consequently, the actual throughput for the M/HG/1/K system is a product of a frame arrival (= departure) rate and non-blocking probability for frames. Now, it is a time to obtain the blocking probability P_B. Fortunately, early researchers, Keilson and Servi, have already established the blocking probability P_B in the finite capacity system which is represented in terms of the probability that an arriving frame finds greater than equal to K frames in the infinite capacity system. [40] Let us now define the notations and their definitions of the equilibrium probabilities for the finite capacity system:

- $p_k{}^*$ *A probability of the number of frames in the finite equilibrium system (k=0,1,2,$\cdots$,K)*
- $r_k{}^*$ *A probability that an arrival finds* k *frames in the finite equilibrium system whether or not they enter the queue (k=0,1,2,$\cdots$,K)*
- $d_k{}^*$ *A probability that a departure leaves* k *frames in the finite equilibrium system (k=0,1,2,$\cdots$,K-1)*
- $r_k{}^{**}$ *A probability that an entering frame (being not blocked) finds* k *frames in the finite equilibrium system (k=0,1,2,$\cdots$,K-1).*

Furthermore, we consider the following relationships. According to the PASTA property [38], we obtain the equality $p_k{}^* = r_k{}^*$. Based on the Burke's theorem [41],

we also acquire the equality ${d_k}^* = {r_k}^{**}$ on average. Thus, for $i < K$, we have

$$ {p_k}^* = {r_k}^* = (1 - P_B){r_k}^{**} = (1 - P_B){d_k}^* \tag{5–42} $$

and

$$ P_B = {p_K}^* = {r_K}^* = 1 - \sum_{k=0}^{K-1} {r_k}^* \tag{5–43} $$

We also know that, on average, the frequency at which frames are allowed to enter the system is equal to the frequency at which frames depart from the system. Thus, we have

$$ \lambda(1 - {p_K}^*) = \frac{1 - {p_0}^*}{E[\widetilde{x}]} \tag{5–44} $$

From Equations (5–42) and (5–43),

$$ \rho(1 - P_B) = 1 - (1 - P_B){d_0}^* \tag{5–45} $$

Therefore,

$$ P_B = 1 - \frac{1}{(\rho + {d_0}^*)} \tag{5–46} $$

If we consider the single step transition probability matrix P^* for the finite capacity (K) system, it must be truncated at $K - 1$ because of its capacity and is given as follows:

$$ P^* = \begin{bmatrix} a_0 & a_1 & a_2 & a_3 & \cdots & 1 - \sum_{k=0}^{K-2} a_k \\ a_0 & a_1 & a_2 & a_3 & \cdots & 1 - \sum_{k=0}^{K-2} a_k \\ 0 & a_0 & a_1 & a_2 & \cdots & 1 - \sum_{k=0}^{K-3} a_k \\ 0 & 0 & a_0 & a_1 & \cdots & 1 - \sum_{k=0}^{K-4} a_k \\ 0 & 0 & 0 & a_0 & \cdots & 1 - \sum_{k=0}^{K-5} a_k \\ \vdots & \vdots & \vdots & \vdots & & \vdots \\ 0 & 0 & 0 & 0 & \cdots & 1 - k_0 \end{bmatrix} \tag{5–47} $$

The only difference between two matrices, P^* and P is after the $(K-1)$th columns, thus the stationary probability equation for a finite capacity system is identical to that of the infinite capacity system up to the state $(K-1)$, which implies that the state probabilities in equilibrium for the finite system and the infinite system are at worst proportional up to the state $(K-1)$. Thus we have

$$d_k{}^* = Cd_k \tag{5–48}$$

and, the probabilities sum to one, so

$$C = \frac{1}{\sum_{j=0}^{K-1} d_j} \tag{5–49}$$

Finally, we have

$$d_k{}^* = \frac{d_k}{\sum_{j=0}^{K-1} d_j} = \frac{d_k}{d_0 + d_1 + d_2 + \cdots + d_{K-1}} = \frac{p_k}{p_0 + p_1 + p_2 + \cdots + p_{K-1}} \tag{5–50}$$

where d_k and p_k is defined in Equation (5–6). Therefore the M/HG/1/K finite capacity system is directly related to the M/HG/1 infinite capacity system. If we want to find p_k (=d_k) which represents the steady-state probability for the infinite capacity system in equilibrium, we can obtain the following.

$$d_k = d_0 a_k + \sum_{j=1}^{k+1} d_j a_{k-j+1} \qquad k = 0, 1, 2, \cdots \tag{5–51}$$

Since a_k, which corresponds to a probability that the random variable $\widetilde{\phi}$ is equal to k, is already defined in Equation (5–7) and can be represented as in Equation (5–17), we

obtain

$$
\begin{aligned}
a_k &= \frac{1}{k!}\frac{d^k}{dz^k}\Phi(z)\bigg|_{z=0} \\
&= \frac{1}{k!}\frac{d^k}{dz^k}F^L_{hygam}(\lambda-\lambda z)\bigg|_{z=0} \\
&= \frac{1}{k!}\frac{d^k}{dz^k}\left[\sum_{i=0}^{N}\alpha_i\beta_i^{k_i}(\beta_i+\lambda-\lambda z)^{-k_i}\right]\bigg|_{z=0} \\
&= \frac{1}{k!}\sum_{i=0}^{N}\alpha_i\beta_i^{k_i}\prod_{j=0}^{k-1}(k_i+j)\,\lambda^k(\beta_i+\lambda)^{-k_i-k} \qquad k>0
\end{aligned}
\tag{5–52}
$$

and

$$
\begin{aligned}
a_0 &= \Phi(z)\big|_{z=0} \\
&= F^L_{hygam}(\lambda-\lambda z)\big|_{z=0} \\
&= \sum_{i=0}^{N}\alpha_i\beta_i^{k_i}(\beta_i+\lambda-\lambda z)^{-k_i}\bigg|_{z=0} \\
&= \sum_{i=0}^{N}\alpha_i\beta_i^{k_i}(\beta_i+\lambda)^{-k_i}
\end{aligned}
\tag{5–53}
$$

If we attempt to find the steady-state probability d_k in Equation (5–51) recursively, then we can obtain the following:

$$
\begin{aligned}
k=0; &\qquad a_0d_1 = (1-a_0)d_0 \\
k=1; &\qquad a_0d_2 = d_1 - a_1(d_0+d_1) \\
k=2; &\qquad a_0d_3 = d_2 - a_1d_2 - a_2(d_0+d_1) \\
k=3; &\qquad a_0d_4 = d_3 - a_1d_3 - a_2d_2 - a_3(d_0+d_1) \\
\vdots &\qquad\qquad \vdots
\end{aligned}
\tag{5–54}
$$

and in general form,

$$
a_0d_{k+1} = \left[1-\sum_{i=1}^{k}a_i\right]\left(\sum_{i=0}^{k}d_i\right) + \sum_{i=2}^{k}d_i\sum_{j=k-i+2}^{k}a_j \tag{5–55}
$$

where d_0 is equal to $1-\rho$, which means that the probability of a departure frame leaves behind zero frames, namely, an empty system.

So far we have all tools required in obtaining throughput and delay for the M/HG/1/K system. The actual arrival rate λ_a (=λ_d) for the M/HG/1/K system is equal to $\lambda(1-P_B)$ as appeared in Equation (5–41) and the probability $(1-P_B)$ is given by $1/(\rho+{d_0}^*)$ from Equation (5–46). In Equation (5–50) we have ${d_0}^* = d_0/\sum_{i=0}^{K-1} d_i$ and we acquire $\sum_{i=0}^{K-1} d_i = \sum_{i=0}^{K-1}\left(d_0 a_i + \sum_{j=0}^{K+1} d_j a_{i-j+1}\right)$ from Equation (5–51). Consequently, we have

$$\lambda_a = \frac{\lambda}{\rho + \frac{d_0}{\sum_{i=0}^{K-1}\left(d_0 a_i + \sum_{j=0}^{K+1} d_j a_{i-j+1}\right)}} \tag{5–56}$$

where a_k and d_k can be obtained from Equation (5–52) to Equation (5–55). In equilibrium, the average number of frames N for the M/HG/1/K system is given

$$\begin{aligned} N &= \sum_{k=0}^{K} k{p_k}^* \\ &= \sum_{k=0}^{K-1} k{p_k}^* + K{p_K}^* \end{aligned} \tag{5–57}$$

From Equations (5–42), (5–43) and (5–46), we have

$$\begin{aligned} N &= \frac{1}{(\rho+{d_0}^*)}\sum_{k=0}^{K-1} k{d_k}^* + KP_B \\ &= \frac{1}{(\rho+{d_0}^*)}\sum_{k=0}^{K-1} k{d_k}^* + K\left[1-\frac{1}{(\rho+{d_0}^*)}\right] \\ &= \frac{\sum_{k=0}^{K-1} k{d_k}^* + K\left[\rho+{d_0}^*-1\right]}{(\rho+{d_0}^*)} \end{aligned} \tag{5–58}$$

The average time spent W in this system can be acquired by using Little's law.

$$W = \frac{N}{\lambda_a} = \frac{\sum_{k=0}^{K-1} k{d_k}^* + K\left[\rho+{d_0}^*-1\right]}{\lambda} \tag{5–59}$$

Let us now define the following notations.

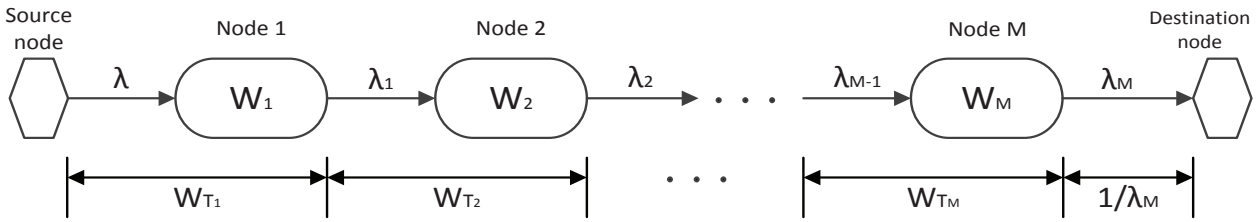

Figure 5-2. Finite capacity network systems based on multimedia traffic after building a routing path.

λ	*Arrival rate to node 1*
λ_i	*Arrival rate to node (i+1) = Departure rate from node i*
W_i	*Average time spent in node i (= queue + service)*
W_{T_i}	*Average time spent from a departure instant at node (i-1) to a departure instant at node i*
P_{B_i}	*Blocking probability at node i*
$\rho_1(=\lambda E[\widetilde{x}])$	*Utilization factor at node 1*
$\rho_i(=\lambda_{i-1}E[\widetilde{x}])$	*Utilization factor at node i*
${d_{i,0}}^*$	*Probability that a departure from node i leaves behind an empty system*
${d_{i,k}}^*$	*Probability that a departure from node i leaves behind k frames in the system*

Therefore, throughput at each node is given as follows:

$$\begin{aligned}
\lambda_1 &= \lambda\left(1-P_{B_1}\right) = \frac{\lambda}{\left(\rho_1+d^*_{1,0}\right)} \\
\lambda_i &= \lambda_{i-1}\left(1-P_{B_i}\right) = \frac{\lambda_{i-1}}{\left(\rho_i+d^*_{i,0}\right)} \\
\lambda_M &= \lambda_{M-1}\left(1-P_{B_M}\right) = \frac{\lambda_{M-1}}{\left(\rho_M+d^*_{M,0}\right)}
\end{aligned} \tag{5–60}$$

and the average time spent from a departure instant at node $(i-1)$ to a departure instant at node i is given as follows:

$$\begin{aligned} W_{T_1} &= \tfrac{1}{\lambda} + W_1 \\ W_{T_i} &= \tfrac{1}{\lambda_{i-1}} + W_i \\ W_{T_M} &= \tfrac{1}{\lambda_{M-1}} + W_M \end{aligned} \tag{5–61}$$

where

$$\begin{aligned} W_1 &= \tfrac{1}{\lambda}\left[\sum_{k=0}^{K-1} k d^*_{1,k} + K\left(\rho_1 + d^*_{1,0} - 1\right)\right] \\ W_i &= \tfrac{1}{\lambda_{i-1}}\left[\sum_{k=0}^{K-1} k d^*_{i,k} + K\left(\rho_i + d^*_{i,0} - 1\right)\right] \\ W_M &= \tfrac{1}{\lambda_{M-1}}\left[\sum_{k=0}^{K-1} k d^*_{M,k} + K\left(\rho_M + d^*_{M,0} - 1\right)\right] \end{aligned} \tag{5–62}$$

Thus the total delay for this system is

$$W_T = \frac{1}{\lambda_M} + \sum_{i=1}^{M} W_{T_i} \tag{5–63}$$

5.4 Results and Discussion

So far, we have studied two types of network systems, M/HG/1 and M/HG/1/K, which have the Hyper-Gamma service time distribution with an infinite capacity and a finite capacity (of size K) in the queue. Moreover, we assume that the arrival process to a network node follows a Poisson process, since we do not have information about the arrival process in real network systems yet. Both systems are considered as a special case of the M/G/1 queueing system and the dynamic behavior of this system can be specified at its imbedded point. (i.e. the departure instant of a frame from the server.) Throughput of the infinite capacity system is equal to the average arrival rate because of the assumption for the arrival process and enough space to accept arriving frames. Total delay is represented in terms of the average arrival rate λ, the first, and second moments of the Hyper-Gamma service time distribution. But, in the finite capacity system, throughput at each node is expressed as a product of the average arrival rate to that node and its non-blocking probability. Furthermore, delay in each node depends on

the total time spent in the previous node and its expression has a quite complicate form as given in Equations from (5–61) to (5–63).

CHAPTER 6
CONCLUSIONS AND FUTURE RESEARCH DIRECTION

6.1 Conclusions

Multimedia traffic has become one of the major sources of network traffic loads due to the massiveness of size. So it is quite cumbersome to analyze and handle its properties. Thus we need an analytical and tractable model to specify its stochastic properties which directly affects the performance of network systems. In this dissertation, the statistical characteristic of multimedia traffic has been studied for how it contributes to dynamic behavior of network systems based on multimedia traffic flows.

As the first step, we have obtained basic elements which consist of multimedia traffic, namely, a stream of frames from commercial DVD movies. Since making a histogram is conventionally a natural and fundamental way of representing a set of empirical data drawn from a real world and one can afford to estimate a statistical characteristic of data with this technique, we build an empirical histogram for a statistical analysis of empirical data. The result of empirical histograms for the multimedia frame size shows that the inherent statistical characteristic is not a unimodal property. Since a mode of histograms is not unique, we interpret these phenomena as a mixture of more than one unimodal distribution which has only one mode. Among these kinds of mixture type distributions, we select the Hyper-Gamma distribution as a candidate model for multimedia traffic because of its versatility. By varying a set of shape and scale parameters, we can obtain the Hyper-Exponential, the Hyper-Erlang, and the Hyper-ChiSquare distributions and, moreover, the Hyper-Exponential and Hyper-Erlang distribution have been introduced in research areas of a performance analysis for wireless communication networks. Consequently, after an examination for the frame size distribution of a large quantity of DVD movies, we are faced with the fact that the statistical model for the frame size distribution contributing to multimedia traffic follows the Hyper-Gamma distribution.

As the next step, we have applied this result to network systems. When we generally attempt to analyze the dynamic behavior of network systems, we need exponential assumptions in an arrival process and a service time distribution to obtain theoretical results. One such network with these assumptions is the Jackson network. Unfortunately, one of these assumptions or both of them seldom happen in a real world and the lack of the exponential assumption makes it difficult in analyzing the network performance. Moreover, we may intuitively know the fact that the service time required for a node to handle movie frames in network systems is proportional to the size of movie frames and also follows the Hyper-Gamma distribution. Thus, we have to find another method, rather than the Jackson's approach, to obtain a performance of such network system based on multimedia traffic. Consequently, we consider a tandem network with some assumptions; i) a routing path has already been established. ii) all nodes in the network system are identical and play a role of a relay center in which they cannot generate their own data frame for multimedia traffic. iii) the arrival process for multimedia traffic follows a Poisson process at a rate of λ frames per second. iv) a type of data flow is one way traffic which means that the traffic stream is one of up-streaming or down-streaming. v) the service discipline follows FIFO service one by one. Therefore we have a tandem network with the M/HG/1 and the M/HG/1/K queueing nodes. As a result, throughput for the infinite capacity system is equal to an average arrival rate to the first node because of the assumption for the arrival process and enough room for an entrance into a node for arriving frames. Total delay is represented in terms of the average arrival rate, the first, and second moments of the Hyper-Gamma service time distribution. In the case of the finite capacity system, throughput at each node is represented in the product form of the average arrival rate to that node and its non-blocking probability. Furthermore, delay in each node depends on the total time spent in the previous node.

6.2 Future Research Direction

If we want to more specifically describe the dynamic behavior of network systems with multimedia traffic in a real world, we need to get rid of the assumptions which are considered. The first assumption is that a routing path has already been established. This implies that a transition probability for a frame from a node to a node is already fixed and is identical to one. If the transition probability is taken into account for the network system, the actual arrival rate to a certain node will be slightly changed since the arrival rate to a certain node in network systems is represented as a product of a departure rate of the previous node and the transition probability from that node to a current node. Generally, this transition probability is related to a Medium Access Control (MAC) in a real world. The second one we have to consider is that each node in the network system works only as a relay center. But the network follows a distributed system or a file sharing architecture, for example, Peer to Peer (P2P) system, we need to consider the queue which is already stored in a certain node. In this case, there are two types of nodes; a node in which has no relayed frames and a node in which has relayed frames. In case of having no relayed frames in a node, the actual arrival rate to the next node is equal to the interarrival time for frames which are already stored in the previous node. In case of a node in which has relayed frames, the actual arrival rate to the next node could be identical to the sum of a product of each probability to transfer a stored frame and to transfer a relayed frame and a frame departure rate from that node.

So far, we have conducted an analysis with a service time distribution from real data and this is not enough to predict a dynamic behavior of the network system because a service process and an arrival process are independent. Therefore, the next assumption we need to consider is that the arrival process for multimedia traffic follows a Poisson process at a rate of λ. Unfortunately, we do not have information about the arrival process in real network systems yet, thus we need to measure the actual arrival rate for multimedia traffic to a certain node in the network system. For this purpose, we need

to obtain an average interarrival time between frames because the average arrival rate is a reciprocal of the average interarrival time. This work could be accomplished by a packet sniffing method such as using a 'scapy' on linux or a commercial traffic analyzing program. Just for a simulation, one simple way of choosing the arrival process is to make use of the event network simulator such as Network Simulator series (i.e. NS2 or NS3) to synthesize the average arrival rate. In this case, we need to take care of the system utilization factor, since the system utilization factor must be less than equal to unity for a system stability. Therefore the average arrival rate must be less than equal to the average service time. Finally, if we consider all situations described in the above, we can predict the dynamic behavior of network systems specified with multimedia traffic more accurately.

REFERENCES

[1] M. Nomura, T. Fujii, and N. Ohta, “Basic characteristics of variable rate video coding in ATM environment,” *Selected Areas in Communications, IEEE Journal on*, vol. 7, pp. 752–760, Jun. 1989.

[2] J. Wu, Y. Chen, and K. Jiang, “Two models for variable bit rate MPEG sources,” *IEICE Trans. Commun.*, vol. E78-B, pp. 737–745, May. 1995.

[3] M. Frey and S. Nguyen-Quang, “A gamma-based framework for modeling variable-rate MPEG video sources: the GOP GBAR model,” *Networking, IEEE/ACM Transactions on*, vol. 8, pp. 710–719, Dec. 2000.

[4] O. Rose, “Statistical properties of MPEG video traffic and their impact on traffic modeling in ATM systems,” in *Local Computer Networks, 1995., Proceedings. 20th Conference on*, pp. 397–406, Oct. 1995.

[5] D. Heyman, A. Tabatabai, and T. Lakshman, “Statistical analysis and simulation study of video teleconference traffic in ATM networks,” in *Global Telecommunications Conference, 1991. GLOBECOM ’91. ’Countdown to the New Millennium. Featuring a Mini-Theme on: Personal Communications Services*, vol. 1, pp. 21–27, Dec. 1991.

[6] D. Heyman, “The GBAR source model for VBR videoconferences,” *Networking, IEEE/ACM Transactions on*, vol. 5, pp. 554–560, Aug. 1997.

[7] M. Lee, *Multimedia traffic modeling and bandwidth allocation in home networks*. PhD thesis, University of Florida, Gainesville, FL, USA, 2004.

[8] F. Fitzek and M. Reisslein, “MPEG-4 and H.263 video traces for network performance evaluation,” *Network, IEEE*, vol. 15, pp. 40 –54, Nov.-Dec. 2001.

[9] M. S. Borella, “Source Models of Network Game Traffic,” *Computer Communications*, vol. 23, no. 4, pp. 403–410, 2000.

[10] Y. Fang, “Hyper-erlang distribution model and its application in wireless mobile networks,” *Wireless Networks*, vol. 7, pp. 211–219, May. 2001.

[11] L. Kleinrock, *Queueing Systems: Theory*, vol. 1 of *A Wiley-Interscience publication*. Wiley, 1976.

[12] P. Orlik and S. Rappaport, “Traffic performance and mobility modeling of cellular communications with mixed platforms and highly variable mobilities,” in *Vehicular Technology Conference, 1997, IEEE 47th*, vol. 2, pp. 587–591, May. 1997.

[13] K. R. Rao and J. J. Hwang, *Techniques and standards for image, video, and audio coding*. Upper Saddle River, NJ, USA: Prentice-Hall, Inc., 1996.

[14] W. Bretl and M. Fimoff, “MPEG-2 Tutorial,” Jan. 2000.

[15] ISO, “Information technology – Generic coding of moving pictures and associated audio information: Video,” *ISO/IEC 13818-2*, 2000.

[16] A. Leon-Garcia and I. Widjaja, *Communication Networks: Fundamental Concepts and Key Architectures*. McGraw-Hill series in computer science, McGraw-Hil, 2006.

[17] J. Mitchell, W. Pennebaker, C. Fogg, and D. LeGall, *MPEG Video Compression Standard*. Chapman and Hall, NY, 1997.

[18] D. Freedman and P. Diaconis, “On the histogram as a density estimator:L2 theory,” *Probability Theory and Related Fields*, vol. 57, pp. 453–476, 1981.

[19] P. Orlik and S. Rappaport, “A model for teletraffic performance and channel holding time characterization in wireless cellular communication with general session and dwell time distributions,” *Selected Areas in Communications, IEEE Journal on*, vol. 16, pp. 788–803, Jun. 1998.

[20] A. R. Liddle, “Information criteria for astrophysical model selection,” *Monthly Notices of the Royal Astronomical Society: Letters*, vol. 377, no. 1, pp. L74–L78, 2007.

[21] D. Pelleg and A. Moore, “X-means: Extending K-means with Efficient Estimation of the Number of Clusters,” in *Proceedings of the Seventeenth International Conference on Machine Learning*, pp. 727–734, Jul. 2000.

[22] W. Stallings, “IEEE 802.11: Wireless LANs from a to n,” *IT Professional*, vol. 6, pp. 32–37, Sep.-Oct. 2004.

[23] “ISO/IEC Standard for Information Technology - Telecommunications and Information Exchange Between Systems - Local and Metropolitan Area Networks - Specific Requirements Part 11: Wireless LAN Medium Access Control (MAC) and Physical Layer (PHY) Specifications (Includes IEEE Std 802.11, 1999 Edition; IEEE Std 802.11A.-1999; IEEE Std 802.11B.-1999; IEEE Std 802.11B.-1999/Cor 1-2001; and IEEE Std 802.11D.-2001),” *ISO/IEC 8802-11 IEEE Std 802.11 Second edition 2005-08-01 ISO/IEC 8802 11:2005(E) IEEE Std 802.11i-2003 Edition*, pp. 1–721, 2005.

[24] “IEEE Standard for Information Technology- Telecommunications and Information Exchange Between Systems - Local and Metropolitan Area Networks- Specific Requirements Part Ii: Wireless LAN Medium Access Control (MAC) and Physical Layer (PHY) Specifications,” *IEEE Std 802.11g-2003 (Amendment to IEEE Std 802.11, 1999 Edn. (Reaff 2003) as amended by IEEE Stds 802.11a-1999, 802.11b-1999, 802.11b-1999/Cor 1-2001, and 802.11d-2001)*, pp. i–67, 2003.

[25] T. Paul and T. Ogunfunmi, “Wireless LAN Comes of Age: Understanding the IEEE 802.11n Amendment,” *Circuits and Systems Magazine, IEEE*, vol. 8, pp. 28–54, quarter 2008.

[26] E. Perahia, “IEEE 802.11n Development: History, Process, and Technology,” *Communications Magazine, IEEE*, vol. 46, pp. 48–55, Jul. 2008.

[27] J. M. Wilson, “The next generation of wireless LAN emerges with 802.11n,” *Technology @Intel Magazine*, pp. 1–8, Aug. 2004.

[28] I. F. Akyildiz, X. Wang, and W. Wang, “Wireless Mesh Networks: A Survey,” *Computer Networks*, vol. 47, no. 4, pp. 445–487, 2005.

[29] T. Liu and W. Liao, “Location-dependent throughput and delay in wireless mesh networks,” *Vehicular Technology, IEEE Transactions on*, vol. 57, pp. 1188–1198, Mar. 2008.

[30] R. Bruno, M. Conti, and E. Gregori, “Mesh networks: commodity multihop ad hoc networks,” *Communications Magazine, IEEE*, vol. 43, pp. 123–131, Mar. 2005.

[31] M. Lee, J. Zheng, Y.-B. Ko, and D. Shrestha, “Emerging standards for wireless mesh technology,” *Wireless Communications, IEEE*, vol. 13, pp. 56–63, Apr. 2006.

[32] S. Faccin, C. Wijting, J. Kenckt, and A. Damle, “Mesh WLAN networks: concept and system design,” *Wireless Communications, IEEE*, vol. 13, pp. 10–17, Apr. 2006.

[33] V. Gambiroza, B. Sadeghi, and E. W. Knightly, “End-to-End performance and fairness in multihop wireless backhaul networks,” in *Proceedings of the 10th annual international conference on Mobile computing and networking*, MobiCom ’04, (New York, NY, USA), pp. 287–301, ACM, 2004.

[34] J. Jun and M. Sichitiu, “Fairness and QoS in multihop wireless networks,” in *Vehicular Technology Conference, 2003. VTC 2003-Fall. 2003 IEEE 58th*, vol. 5, pp. 2936–2940, Oct. 2003.

[35] J. F. Lee, W. Liao, and M. C. Chen, “An incentive-based fairness mechanism for multi-hop wireless backhaul networks with selfish nodes,” *Wireless Communications, IEEE Transactions on*, vol. 7, pp. 697–704, Feb. 2008.

[36] J. R. Jackson, “Networks of Waiting Lines,” *Operations Research*, vol. 5, pp. 518–521, Aug. 1957.

[37] J. R. Jackson, “Jobshop-Like Queueing Systems,” *Management Science*, vol. 50, no. 12 supplement, pp. 1796–1802, 2004.

[38] R. W. Wolff, “Poisson arrivals see time averages,” *Operations Research*, vol. 30, pp. 223–231, Mar.-Apr. 1982.

[39] D. Gross, J. Shortle, J. Thompson, and C. Harris, *Fundamentals of Queueing Theory*. Wiley Series in Probability and Statistics, John Wiley & Sons, 2011.

[40] J. Keilson and L. D. Servi, “The M/G/1/K blocking formula and its generalizations to state-dependent vacation systems and priority systems,” *Queueing Systems*, vol. 14, pp. 111–123, 1993.

[41] P. J. Burke, “The Output of a Queuing System,” *Operations Research*, vol. 4, pp. 699–704, Dec. 1956.

BIOGRAPHICAL SKETCH

Kyungwoo Kim received the B.S. degree in electrical and computer engineering from Kyungpook National University, Daegu, South Korea, in 2000, the M.S. degrees in electrical and computer engineering from Kyungpook National University, Daegu, South Korea, in 2002, and University of Florida, Gainesville, Florida, USA, in 2005, respectively. During his Ph.D. career, he participated in the Program Committee of the 15th World Multi-Conference on Systemics, Cybernetics and Informatics, Reviewer of the IEEE International Symposium on Power Line Communications and Its Applications, and Reviewer of the World Multi-Conference on Systemics, Cybernetics and Informatics. His research interests are network traffic modeling and analysis, network routing algorithm, and P2P network.